SUPERCONDUCTIVE TUNNELLING MEASUREMENTS

SUPERCONDUCTIVE TUNNELLING MEASUREMENTS ON THIN FILMS

By

ROBERT CARR DYNES, B.Sc.

A Thesis

Submitted to the Faculty of Graduate Studies

in Partial Fulfilment of the Requirements

for the Degree

Master of Science

McMaster University

October 1965

MASTER OF SCIENCE (1965)
(Physics)

McMASTER UNIVERSITY
Hamilton, Ontario

TITLE: Superconductive Tunnelling Measurements on Thin Films

AUTHOR: Robert Carr Dynes, B.Sc. (University of Western Ontario)

SUPERVISOR: Professor C. K. Campbell

NUMBER OF PAGES: vi, 60

SCOPE AND CONTENTS:

A cryostat to study superconducting thin films using the electron tunnelling technique has been built. In addition, the electronics to study the current voltage characteristics and derivatives thereof of superconductor-insulator-superconductor sandwiches has been constructed and the advantages and limitations of this method of investigation have been outlined.

The characteristics of superconducting lead and various alloys of lead bismuth have been examined and reported. Suggestions for further experiments have been made.

ABSTRACT

The properties of superconducting lead have been studied using the technique of electron tunnelling through a thin insulating barrier. Certain features in the second derivative of the current-voltage characteristic of this tunnelling mechanism have been related to the phonon spectrum of lead.

In addition, a small amount of bismuth impurities have been added and the effect of these impurities on the superconducting density of states reported. In particular, both the superconducting energy gap has widened and the phonon spectrum of lead altered with the addition of these impurities.

ACKNOWLEDGEMENTS

The author wishes to express his gratitude for the continued guidance and encouragement from Dr. C. K. Campbell, and for the advice and suggestions of Mr. D. G. Walmsley without which much time would have been lost. For a bursary and most of the instruments which made this investigation possible, the author is deeply indebted to the National Research Council of Canada.

TABLE OF CONTENTS

I. INTRODUCTION

1.1 Historical

The phenomenon of superconductivity was discovered in 1911 by Kammerlingh Onnes (O1) at Leiden while studying the decrease in resistance of metals as they were cooled. He found that the resistance of certain metals at a characteristic temperature, dropped to zero. Since that time, this peculiar habit of some materials has been extensively studied and many theories as to its cause have been proposed.

Before the era of the quantum theory, attempts were made to describe the behaviour of superconductors in terms of phenomenological theories. The most successful of these theories have been the two fluid model of Gorter and Casimir (G1) which accounts for the thermodynamic properties, and the London equations, developed by Fritz and Heinz London (L1), which account for the electromagnetic properties of a superconductor. The two-fluid model assumes that a percentage of the available conduction electrons are "condensed" into their ground state and these are the superconducting electrons, while the remaining electrons stay in the normal state. It is assumed that these two fluids permeate one another. The London equations, on the other hand describe the infinite conductivity as well as the perfect diamagnetic nature of the superconductor.

The major problem toward the development of a successful

microscopic theory was the lack of knowledge of the interactions between electrons. Fröhlich (F1) first studied the interaction of the electrons in a metal with the acoustic lattice vibrations. From this study he concluded that this interaction would lead to an attraction between electrons near the Fermi surface. Later, Cooper (C1) showed that the attractive force between two electrons at the Fermi surface is mediated by the phonons. This conclusion led Bardeen, Cooper and Schrieffer (known as BCS) to propose a microscopic theory of superconductivity that agrees amazingly well with experiment (B1).

One of the most conclusive endorsements of the BCS theory showed up in the results of an experiment performed by Giaever (G2) using the phenomenon of quantum mechanical tunnelling. In this experiment, electrons were allowed to tunnel from one metal, through a thin insulating barrier into another metal. Either or both of these metals could be superconducting. These experiments using this technique have verified many of the predictions of the BCS theory of superconductivity. In particular, this method has become an extremely useful tool in studying the density of states of electrons, both in the region of the Fermi surface, and as distantly removed as a few $k\,\theta_D$ (θ_D = the Debye temperature) from the Fermi surface. It has been found that the coupling of the electrons and phonons is so strong that the density of states is altered enough to make this effect observable using the tunnelling technique.

1.2 Purpose of this Thesis

The purpose of this thesis is to describe a method by which the density of states of a superconductor and the effects of the phonons

on that density of states is observed. Essentially the experiment consists of obtaining the second derivative $(\frac{d^2I}{dV^2})$ of the I-V (current vs. voltage) tunnelling characteristic curve of two similar superconductors separated by a thin insulating barrier. In this case, that barrier is the oxide of the material used as the superconductor. The method by which these tunnelling junctions are produced is described and the method used to differentiate the I-V characteristic is outlined in some detail.

In addition, a small amount of impurity is added and the effect of this on both the energy gap of the superconductor and the density of states in the phonon-affected region is reported. In particular, five and ten per cent impurities of bismuth in lead are studied and the results are given. It is felt that the existing data on lead bismuth alloys is incomplete and an extension of the knowledge would prove valuable.

Also, an experiment designed to investigate the properties of bulk mercury using this tunnelling technique is described and the probable reasons for its failure are outlined.

II. THEORY

2.1 The Gorter-Casimir Theory

The two fluid model of superconductivity as postulated by Gorter and Casimir (G1) gives a useful picture of the transition from normal to superconducting state. They postulated that below a certain temperature T_c (the critical temperature), the available electrons could be separated into two classes. Firstly, a fraction of them ϕ remained normal and underwent no change. The others $(1-\phi)$, they claimed, condensed into the superconducting state. Following this assumption, and the assumption that at $T = T_c$ $\phi = 1$

and at $T = 0$ $\phi = 0$,

a rather arbitrary expression for the free energy of the system was developed

$$F_{TOT} = \phi^x F_N(T) + (1-\phi) F_S(T) \qquad (1)$$

where $F_N(T) = -\frac{1}{2}\gamma T^2$ (the usual expression for a normal metal)

and $F_S(T) = -\beta$ = a constant.

Experimentally it was found that $x \approx \frac{1}{4}$. This was chosen for no other reason than that it agreed with experimental results.

Minimizing equation (1) and fitting to the appropriate boundary conditions leads to the result

$$\phi = (T/T_c)^4.$$

In other words the number of superconducting electrons increases quite rapidly as the temperature is lowered below T_c.

This theory leads to rather good qualitative agreement with

experiment, predicting the electronic specific heat in the superconducting state and an expression for the critical magnetic field as a function of temperature.

2.2 The London Theory

In 1933 Meissner and Ochsenfeld (M1) discovered that a superconductor is a perfect diamagnet. That is, a magnetic field impressed on the material penetrates only a very small distance into the superconductor (about 500 A°). Their results also showed that even if the field is already inside the metal before cooling through T_c, the flux is actually expelled as the material becomes superconducting. Hence a superconductor is more than just a perfect conductor.

This fact, as well as the perfect conductivity of a superconductor led F. and H. London to develop the now-famous London equations (L1).

Starting with the vector potential $\bar{A}$ and bearing in mind the Meissner effect the Londons developed the first of their equations

$$\bar{B} = -\Lambda(\nabla \times \bar{J}) \text{ or } \bar{J} = -\frac{1}{\Lambda}\bar{A} \qquad (2)$$

where: $\bar{J}$ = superconducting current density

$\bar{B}$ = impressed magnetic field

Λ = a constant whose value

is characteristic of the superconductor. If all the conduction electrons were allowed to accelerate freely Λ would have the value $\frac{m}{ne^2}$

where: m = electronic mass

e = electronic charge

n = number of conduction electrons

From this equation it is possible to obtain an expression for the magnetic field inside a superconductor. In the one dimensional case

$$\bar{B}_{INT} = B_{EXT}\, e^{-\frac{x}{\lambda}} \qquad (3)$$

$$\text{where} \quad \lambda = \sqrt{\frac{\Lambda}{\mu}} .$$

This λ is defined as the penetration depth.

Since the current is superconducting, the Londons assumed that there is no collision with the lattice (i.e., no resistance and hence the force on an electron would be the same as if it were accelerating freely in an applied field). Hence, the force on the electron

$$\bar{F} = e\bar{\mathcal{E}} = m\bar{v}$$

$$\therefore \bar{\mathcal{E}} = \frac{m}{e}\bar{v} .$$

But $\bar{J}_s = n e \bar{v}$ superconducting current density

$$\therefore \bar{\mathcal{E}} = \frac{m}{ne^2}\dot{\bar{J}}_s = \Lambda\, \dot{\bar{J}}_s . \qquad (4)$$

This equation is the second of the London equations and accounts for the perfect conductivity of a superconductor. Applying these two equations, it is found that one can explain many of the phenomena associated with superconductors, including the Meissner effect, frequency dependence of a superconductor and the recently observed (D1)(D2) quantization of flux in a superconductor.

2.3 Pippard's Extension of the London Theory

Pippard (P1) suggested a modification to the London equations to explain certain experimental results. It was found that the penetration depth λ began to increase quite appreciably when impurities

were added which lowered the electronic mean free path. In the London theory no such an effect was expected since Λ depended only on the constants of the material. Also, variation of the penetration depth with angle between the surface of a sample and the crystal axes was observed. These discrepancies led Pippard to propose a non-local modification of the London equations with a characteristic coherence length $\xi_0 \approx 10^{-4}$ cms. This non-local development implies that we must consider more than just nearest neighbour interactions, and that the superconducting electron is "aware" of events occurring over a rather large spatial region. Consequently Pippard identified a parameter with the range of coherence of the pure superconductor and defined a coherence distance $\xi(l)$ such that

$$\frac{1}{\xi(l)} = \frac{1}{\xi_0} + \frac{1}{\alpha l} \qquad (5)$$

where l = mean free path of electron

α = a constant ≈ 1

In the BCS theory this ξ_0 is a measure of the size of the pair bound state from which the super fluid wave function is constructed.

The form of this expression suggests that

$$\xi(l) \to \xi_0 \qquad \text{as} \qquad l \to \infty$$

$$\text{and} \quad \xi(l) \to l \qquad \text{as} \qquad l \to 0$$

In addition Pippard altered the London equation

$$\bar{J}_s = -\frac{1}{\Lambda}\bar{A}$$

$$\text{to} \qquad \bar{J}_s(\bar{r}) = -\frac{3}{\xi_0 \Lambda}\int \frac{\bar{R}\left[\bar{R}\cdot\bar{A}(\bar{r}')\right] e^{-\bar{R}/\xi(l)}}{\bar{R}^4} d^3\bar{r}'$$

$$\text{where} \qquad \bar{R} = \bar{r} - \bar{r}'$$

in an exactly analogous manner to the replacing of Ohm's law by Chambers' (C2) non-local expression used to describe the anomolous skin effect.

Although these phenomenological theories describe in an adequate manner the existing data, they do not give us much of an indication of the microscopic nature of superconductivity and the mechanism which causes it.

2.4 The Microscopic Theory of Superconductivity

It was pointed out by Frohlich (F1) that an electron in a lattice is screened by a cloud of virtual phonons. These are called virtual phonons due to the fact that, because of the very short lifetime of them, and because of the uncertainty principle, energy need not be conserved. Now consider an interaction between two electrons as illustrated in figure 1.

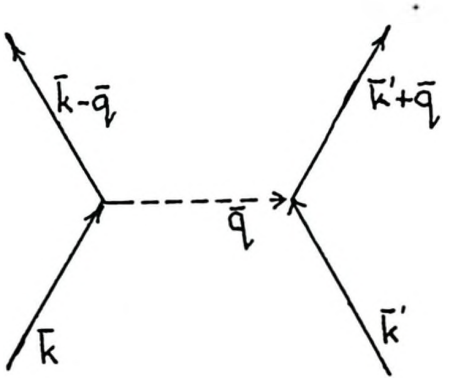

Figure 1

An electron of wave vector $\bar{k}$ emits a virtual phonon $\bar{q}$ which is adsorbed by another electron $\bar{k}'$ thus leaving electrons in the final state $\bar{k} - \bar{q}$ and $\bar{k}' + \bar{q}$. As stated earlier, this process need not be a conservative one. In fact the effective matrix element for this sort of interaction could be written (T1)

$$V_{kk'} = \frac{2\hbar\omega_q |M_q|^2}{(\mathcal{E}_{k'} - \mathcal{E}_{k'q})^2 - (\hbar\omega_q)^2} \tag{6}$$

where $\hbar\omega_q$ = phonon energy

$\mathcal{E}_{k'}$ = electron energy measured from the Fermi surface

M_q = a matrix element for a single scattering by the electron-phonon coupling.

It should be noticed that near the Fermi surface, where $\mathcal{E}_{k'} \lesssim k\,\Theta_D$, the term is negative and roughly equal to

$$V_{kk'} = -\frac{2\,|M_q|^2}{\hbar\omega_q} \tag{7}$$

Hence we see that under these circumstances the interaction is indeed an attractive one. The BCS theory is based on the postulate that when this attractive interaction dominates the normal coulombic repulsion, superconductivity results. Cooper (C1) showed that however small this net attraction is between two electrons just above the Fermi surface, the result is that these electrons could form a bound state. The electrons undergoing this interaction must be within a distance $\hbar\omega_q$ of the Fermi surface.

Considering all possible interactions which take a pair of electrons from any two $\bar{k}$ values in this region to any other two, it is

found that because of alternating signs of matrix elements, the total interaction energy is negligible. If however, one categorizes all possible $\bar{k}$ values into pairs, and further demands that neither or both states of a given pair be occupied, one finds that the matrix elements have all the same sign and the total interaction energy is not negligible. Hence we can say that a pair $(\bar{k}_1,\bar{k}_2)$ scatters into another state $(\bar{k}_1',\bar{k}_2')$. Because we must conserve momentum

$$\bar{k}_1 + \bar{k}_2 = \bar{k}_1' + \bar{k}_2' = \bar{K}$$

The most favourable arrangement which satisfies this condition is that in which $\bar{K} = 0$, i.e., $\bar{k}_1 = -\bar{k}_2$. It is also more favourable that these electrons have equal and opposite values of spin. Hence we can write the interaction as $(\bar{k}\uparrow,-\bar{k}\downarrow)$ scattering into $(\bar{k}'\uparrow,-\bar{k}'\downarrow)$. This also satisfies the all-important condition that a finite amount of energy is needed to excite a single unpaired or normal electron for, in order to have a single electron in a state $\bar{k}$, we must remove from the system a large number of possible interactions of other states with the state $(\bar{k}\uparrow,-\bar{k}\downarrow)$. Thus the total energy difference between having all pairs and having a single excited electron is a multiple of many single pair correlation energies. This consideration accounts for, in a qualitative way, the energy gap in the density of states curve characteristic of a superconductor.

It should be pointed out, however, that this correlation energy is very small compared to most other interactions contributing to the total energy of the electrons. The BCS theory assumes that all these other interactions are the same for the superconducting state as for

the normal state. Hence the energy difference between the superconducting state and the normal state is this correlation energy.

The BCS theory, in calculating the ground state of a superconductor, assumes that the energy is due to the correlation of these Cooper pairs of opposite spin and momentum and the screened coulomb energy. The matrix element for transforming a pair in the state $(\bar{k}\uparrow,-\bar{k}\downarrow)$ into the state $(\bar{k}'\uparrow,-\bar{k}'\downarrow)$ can be written

$$V_{kk'} = -2 \left\langle -\bar{k}'\downarrow, \bar{k}'\uparrow \left| H \right| -\bar{k}\downarrow, \bar{k}\uparrow \right\rangle$$

where H is a Hamiltonian in which all the common terms between the normal and superconducting states have been omitted. From equations (6) and (7) we see that $V_{kk'}$ is approximately a constant and so we say that

$$V_{kk'} \approx V \text{ for } \mathcal{E}_k, \mathcal{E}_{k'} \leq \hbar\omega_q \qquad (8)$$

$$V_{kk'} = 0 \text{ elsewhere.}$$

Recall that a necessary condition for superconductivity is that $V < 0$. If we define h_k to be the probability that the $(\bar{k}\uparrow,-\bar{k}\downarrow)$ is occupied, then the energy of the superconducting ground state as compared to the normal ground state at $0^{\circ}K$ is

$$W(0) = \sum_k 2\,\mathcal{E}_k h_k - \sum_{kk'} V_{kk'} \left\{ h_k(1-h_{k'})\, h_{k'}\,(1-h_k) \right\}^{\frac{1}{2}}.$$

Applying equation (8) we see that

$$W(0) = \sum_k 2\,\mathcal{E}_k h_k - V \sum_{k'k} \left\{ h_k(1-h_{k'})\, h_{k'}\,(1-h_k) \right\}^{\frac{1}{2}}. \qquad (9)$$

The first term in this expression is the difference between the kinetic

energy of the system in the superconducting and normal states at $0^{\circ}K$. This is very small compared with the second term which gives the correlation energy for all possible transitions from $(\bar{k}\uparrow,-\bar{k}\downarrow)$ to $(\bar{k}'\uparrow,-\bar{k}'\downarrow)$. To be in the superconducting state W(0) must be negative. Hence minimizing (9) with respect to h_k gives

$$\frac{\left[h_k(1-h_k)\right]^{\frac{1}{2}}}{1-2h_k} = V \frac{\sum_{k'}\left[h_{k'}(1-h_{k'})\right]^{\frac{1}{2}}}{2\,\mathcal{E}_k} . \tag{10}$$

If we define

$$\Delta = V\sum_{k'}\left[h_{k'}(1-h_{k'})\right]^{\frac{1}{2}} \tag{11}$$

which turns out to be the energy gap parameter for the k'th electron, equation (10) becomes

$$h_k = \tfrac{1}{2}\left(1 - \frac{\mathcal{E}_k}{E_k}\right) \tag{12}$$

where

$$E_k = (\mathcal{E}_k^{\,2} + \Delta^2)^{\frac{1}{2}} . \tag{13}$$

which gives, for equation (11)

$$\Delta = \frac{V}{2}\sum_{k}\frac{\Delta}{(\mathcal{E}_k^{\,2} + \Delta^2)^{\frac{1}{2}}} .$$

Assuming that Δ is approximately constant for $\mathcal{E}_k \leq \hbar\omega_q$ and replacing the summation by an integral over energy we obtain

$$\frac{1}{N(0)V} = \int_0^{\hbar\omega_q}\frac{d\mathcal{E}}{\sqrt{\mathcal{E}^2 + \Delta^2}} \tag{14}$$

where N(0) = density of states in the energy region considered = a constant.

This equation has the solution

$$\Delta = \frac{\hbar\omega_q}{\sinh\left[1/N(0)V\right]} \approx 2\hbar\omega_q e^{-\frac{1}{N(0)V}} \tag{15}$$

which, applying back to equation (9) gives us for the ground state energy

$$W(0) = \frac{-2\,N(0)\,(\hbar\omega_q)^2}{\exp\left[2/N(0)V\right]-1}\,.$$

Raising the temperature above $0^{\circ}K$ will result in an increasing number of electrons being excited into single quasi-particle states. These are similar to electrons in a normal metal and will be called normal electrons.

If we define

a_k = probability of occupation of $\bar{k}\uparrow$ or $-\bar{k}\downarrow$ by a single normal electron,

$(1-2a_k)$ = probability that neither $\bar{k}\uparrow$ or $-\bar{k}\downarrow$ are occupied,

W(T) will be a sum of two terms, one a kinetic energy term, and the other a correlation energy term. The free energy expression is

$$G = W(T) - TS = W(T)_{KE} + W(T)_{CORR} - TS \qquad (16)$$

$$W(T)_{KE} = 2\sum_{k} |\varepsilon_k| \left[a_k + (1-2a_k)h_k\right]$$

$$W(T)_{CORR} = -V \sum_{kk'} \left\{ h_k(1-h_{k'})h_{k'}(1-h_k)\right\}^{\frac{1}{2}} \left\{(1-2a_k)(1-2a_{k'})\right\}.$$

The second curly bracket assures that the correlated states are not occupied by normal electrons. Working through a similar analysis as before one obtains an expression for the energy gap

$$\Delta(T) = V \sum_{k'} \left[h_{k'}(1-h_{k'})\right]^{\frac{1}{2}} (1-2a_{k'}) \qquad (17)$$

$$\text{where again } E_k = \left[\varepsilon_k^{\,2} + \Delta^2(T)\right]^{\frac{1}{2}}.$$

Minimizing (16) with respect to a_k yields

$$a_k = \left[\exp\left(E_k/k_BT\right) + 1\right]^{-1}. \qquad (18)$$

In a precisely similar manner as previously, changing (17) from a summation to an integral and imposing (18) one obtains

$$\frac{1}{N(0)V} = \int_0^{\hbar\omega_q} \frac{\tanh\left\{(\varepsilon^2 + \Delta^2(T))^{\frac{1}{2}}/2kT\right\}}{(\varepsilon^2 + \Delta^2(T))^{\frac{1}{2}}}\, d\varepsilon \,. \qquad (19)$$

One should note that at $T = 0$ this expression reduces to (14). It is also important to note that at $T = T_c$, $\Delta \to 0$ and for $T > T_c$ there is no solution and the metal reverts to the normal situation with no energy gap. To find the critical temperature T_c one simply substitutes $\Delta = 0$ in (19) which gives, for $k_B T << \hbar\omega_q$

$$k_B T_c = 1.14\, \hbar\omega_q \exp\left[-1/N(0)V\right]$$

which together with (15) gives

$$2\Delta(0) = 3.52\, k_B T_c \,. \qquad (20)$$

2.5 Density of States

Because the excitations in the superconducting state have a one to one correspondence with Bloch states in a normal metal, the density of states function can be calculated

$$N(E) = N(\varepsilon)\frac{d\varepsilon}{dE} = \frac{N(0)}{dE/d\varepsilon}$$

but applying (13) gives

$$N(E) = N(0)\frac{E}{(E^2 - \Delta^2)^{\frac{1}{2}}} \text{ for } E \geq \Delta \qquad (21)$$

$$= 0 \qquad E < \Delta \text{ (no solution)}.$$

This density of states is shown schematically in figure 2. For energies well above the gap energy this reduces properly to $N(0)$ but at the edge

FIGURE 2

BCS SUPERCONDUCTING DENSITY OF STATES

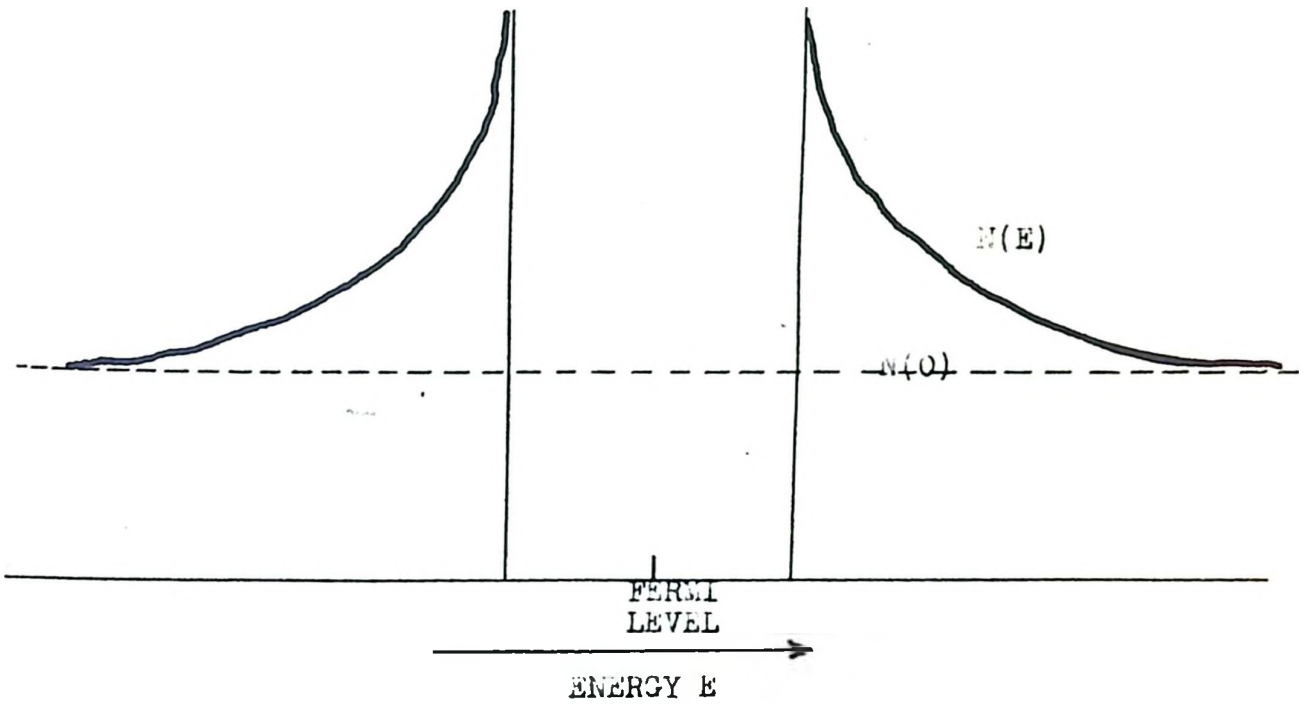

of the gap it is infinite. Crudely, one could say that the states have been piled up at the edge of the gap. This density of states curve leads to a model somewhat analogous to that of an intrinsic semiconductor. In fact this semiconductor model has been used with a relatively high degree of success.

More recently, Schrieffer, Scalapino and Wilkins (S1) have developed a more complicated equation for a complex energy gap function in terms of phonon energies

$$\Delta(\hbar\omega_q) = \Delta_1(\hbar\omega_q) + i\Delta_2(\hbar\omega_q).$$

Assuming a very simple model for the phonon spectrum of lead, (the sum of two Lorentzians centred at the energies $\hbar\omega^1 = 8.5 \times 10^{-3}$ eV (longitudinal phonons) and $\hbar\omega^t = 4.4 \times 10^{-3}$ eV (transverse phonons) with half widths 0.5×10^{-3} eV and 0.75×10^{-3} eV respectively) they calculated that at energies of $\hbar\omega^l + \Delta$ and $\hbar\omega^t + \Delta$ the peaks in the phonon spectrum produce a rapid increase in the imaginary part Δ_2 which corresponds to a drop in the lifetime of the electron excitation. This brings about a corresponding drop in Δ_1. The net effect is to produce a rather sharp drop in the density of states curve $N(E)$ at these energies. In other words, the lifetime of an excited state is proportional to the density of phonons available and the density of final single particle states. As equation (21) indicates, the density of states is sharply peaked at the energy Δ in a superconductor. Hence if there is a concentration of phonons at $\hbar\omega$, those excited states at energy $\hbar\omega + \Delta$ will decay quickly to their final states around the gap. This effect was first reported by Giaever, Hart and Megerle (G3) and

later in a more detailed fashion by Rowell, Anderson and Thomas (R1).

2.6 Electron Tunnelling Between Superconductors

In 1960 Giaever (G2) proposed and carried out the first experiments on the tunnelling of electrons from normal metals into superconductors. Techniques have improved so greatly since then that it has now become as extremely effective tool in measuring the energy gap and density of states in a superconductor.

If one has a sandwich of two metals separated by a thin ($\approx$20 A°) insulating barrier and a potential is applied across that barrier, a current will flow through the barrier by means of quantum mechanical tunnelling of electrons. Depending upon the state of the two metals, i.e., whether they are superconducting or normal, the shape of the resulting I-V curve will vary. Figure 3 illustrates different curves under different circumstances. A brief analysis by means of the accompanying "semiconductor model" diagrams should explain the various details of the different characteristic curves. One should use this model with a certain amount of caution. The validity of this model is discussed by Bardeen (B2).

When no potential is applied across the barrier, the two Fermi levels will line up at the same energy. The application of a potential V will cause the Fermi level of one metal to shift an energy eV with respect to the other one. Assuming the "golden rule" we can say that the transition probability of tunnelling from an occupied state in metal 1 to an unoccupied state in metal 2 can be written

$$P_{12} = \frac{2\pi}{\hbar} \left|M_{12}\right|^2 N_2(E)\,(1-f_2(E))$$

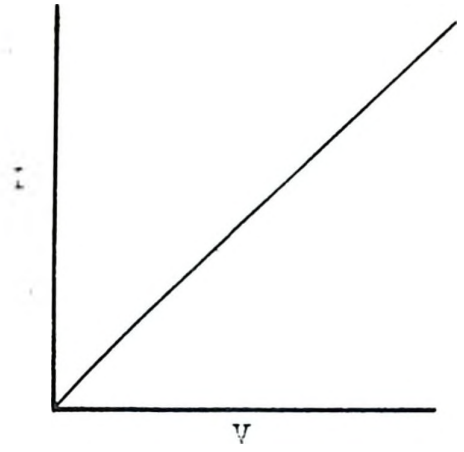

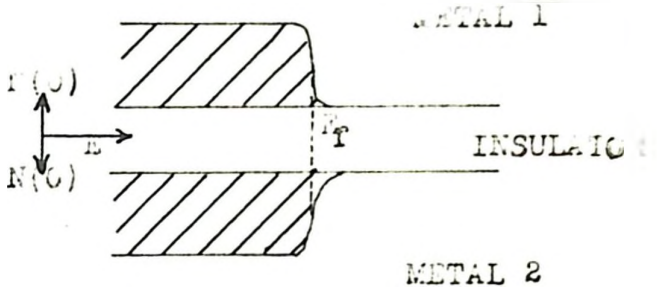

(i) BOTH METALS NORMAL

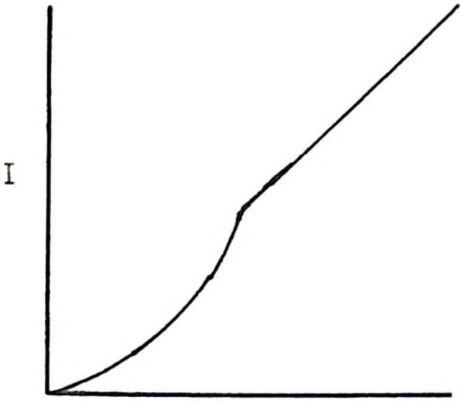

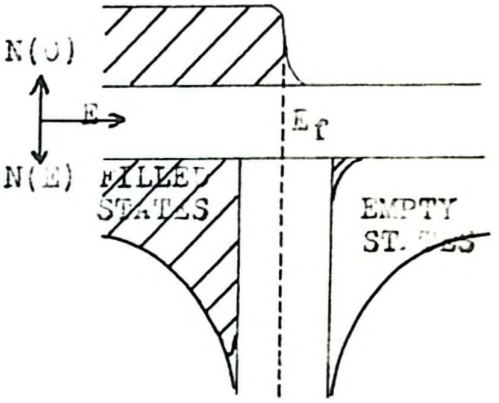

(ii) ONE METAL SUPERCONDUCTING

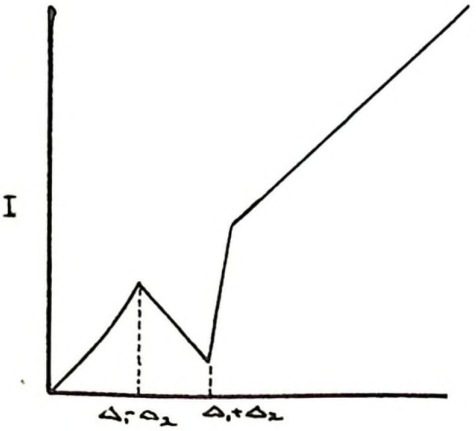

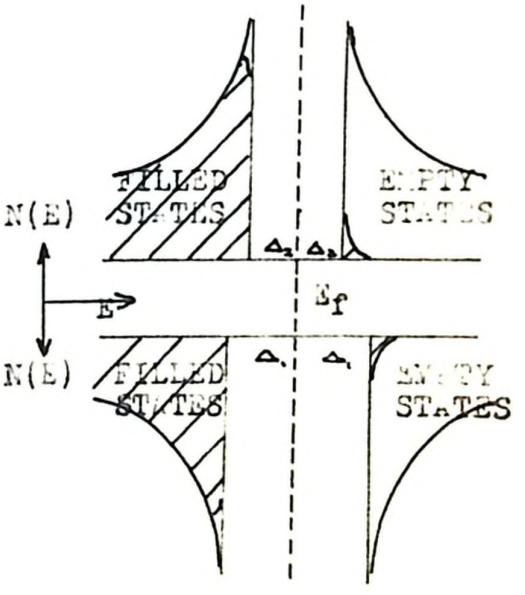

(iii) BOTH METALS SUPERCONDUCTING

where $N_2(E)$ = density of states in metal 2

$f_2(E)$ = Fermi function

M_{12} = transition matrix connecting the two states.

Consequently, the total current tunnelling from metal 1 to metal 2 is the sum of all these transitions. Defining a reduced density of states $\varrho(E) = \frac{N(E)}{N(0)}$

$N(0)$ = density of states in normal metal,

we obtain the expression for current tunnelling from metal 1 to metal 2

$$I_{12} = N_1(0)\, N_2(0)\, \frac{2\pi e}{\hbar} \int_{-\infty}^{\infty} |M_{12}|^2\, \varrho_2(E-eV) \left[1-f(E-eV)\right] \varrho_1(E)\, f(E)\,dE.$$

Similarily in the other direction, the current going from metal 2 to metal 1 can be written

$$I_{21} = N_1(0)\, N_2(0)\, \frac{2\pi e}{\hbar} \int_{-\infty}^{\infty} |M_{21}|^2\, \varrho_2(E-eV) f(E-eV)\, \varrho_1(E) \left[1-f(E)\right] dE.$$

Summing these two we obtain the total current (assuming $|M_{12}| = |M_{21}|$)

$$I_{TOT} = \frac{2\pi e}{\hbar} N_1(0)\, N_2(0) \int_{-\infty}^{\infty} |M_{12}|^2\, \varrho_1(E) \varrho_2(E-eV) \left[f(E-eV)-f(E)\right] dE. \quad (22)$$

Now consider the various possibilities of normal and superconducting metals in figure 3 and assume that $|M_{12}|^2$ is a constant over the range considered.

Case (i). Both metals normal.

In this case $\varrho_1(E) = \varrho_2(E) = 1$ and equation (22) becomes

$$I = \frac{2\pi e^2}{\hbar} N_1(0)\, N_2(0)\, |M_{12}|^2\, V$$

$$\text{or } I = \sigma_N V$$

where σ_N is approximately a constant.

Hence for small applied voltages, the curve produced when both metals are normal is linear.

Case (ii).

If we have the case of one metal normal and one metal superconducting, then

$$\rho_1(E) \neq 1$$

$$\rho_2(E) = 1 \quad \text{and the current becomes}$$

$$I = \frac{\sigma_N}{e} \int_{-\infty}^{\infty} \rho_1(E) \left[f(E-eV) - f(E) \right] dE \ .$$

At $0^\circ K$ this becomes

$$I = \frac{\sigma_N}{e} \int_{-eV}^{eV} \rho_1(E) dE \ . \qquad (23)$$

Differentiating once, we obtain

$$\frac{dI}{dV} = \sigma_N \rho_1(E) \ .$$

Thus we see that by differentiating the I-V characteristic curve at $0^\circ K$ we can obtain directly the density of states of the superconductor. At finite temperatures this becomes slightly more complicated;

$$\frac{dI}{dV} = \sigma_N \int_{-\infty}^{\infty} \rho_1(E) \left\{ \frac{e^{\frac{E-eV}{kT}} \Big/ kT}{\left[e^{\frac{E-eV}{kT}} + 1 \right]^2} \right\} dE. \qquad (24)$$

This is identical to equation (23) except that the term in the curly brackets is a bell-shaped curve that becomes a delta function at $0^\circ K$. Hence at $0^\circ K$ (24) reduces to (23) and at very low temperatures we can say that $\frac{dI}{dV}$ gives us approximately the density of states.

Case (iii).

When both metals are superconducting we have the case that

$$\rho_1(E) \neq 0$$
$$\rho_2(E) \neq 0$$

and the current becomes

$$I = \frac{\sigma_N}{e} \int_{-\infty}^{\infty} \rho_1(E)\, \rho_2(E-eV) \left[f(E-eV) - f(E) \right] dE.$$

Here at $0^{\circ}K$, the derivative $\frac{dI}{dV}$ will give us a measure of the product of the density of states of the two materials. Hence it seems immediately obvious that it would be advantageous to use two superconductors of the same material. In this way, any finer detail would become more apparent.

There is another distinct advantage in using two metals in the superconducting state in these electron tunnelling experiments. Essentially what one is doing is probing one density of states function with another. If a normal metal is used to probe a superconductor, even at $1^{\circ}K$ there is a considerable amount of thermal smearing at the Fermi level as determined by the Fermi function (see figure 4a). In other words, the probe being used is not a sharp one and hence the detail sought after is thermally smeared. On the other hand, using another superconductor circumvents this problem. From equation (21) we see that the edge of the gap, as well as having a large number of available states for tunnelling, is infinitely sharp. Also, if we are well below the critical temperature the number of filled states above the energy gap will be very small (see figure 4b). Consequently it is far more advantageous to probe a density of states

FIGURE 4

SUPERCONDUCTING DENSITY OF
STATES COMPARED TO NORMAL METAL DENSITY OF STATES

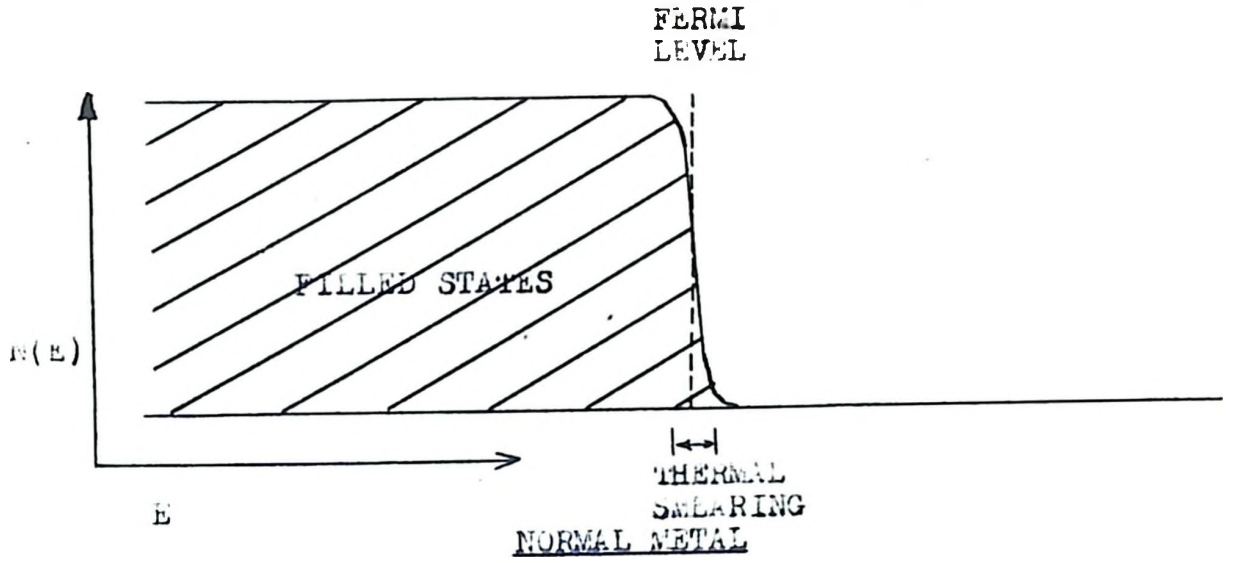

NORMAL METAL

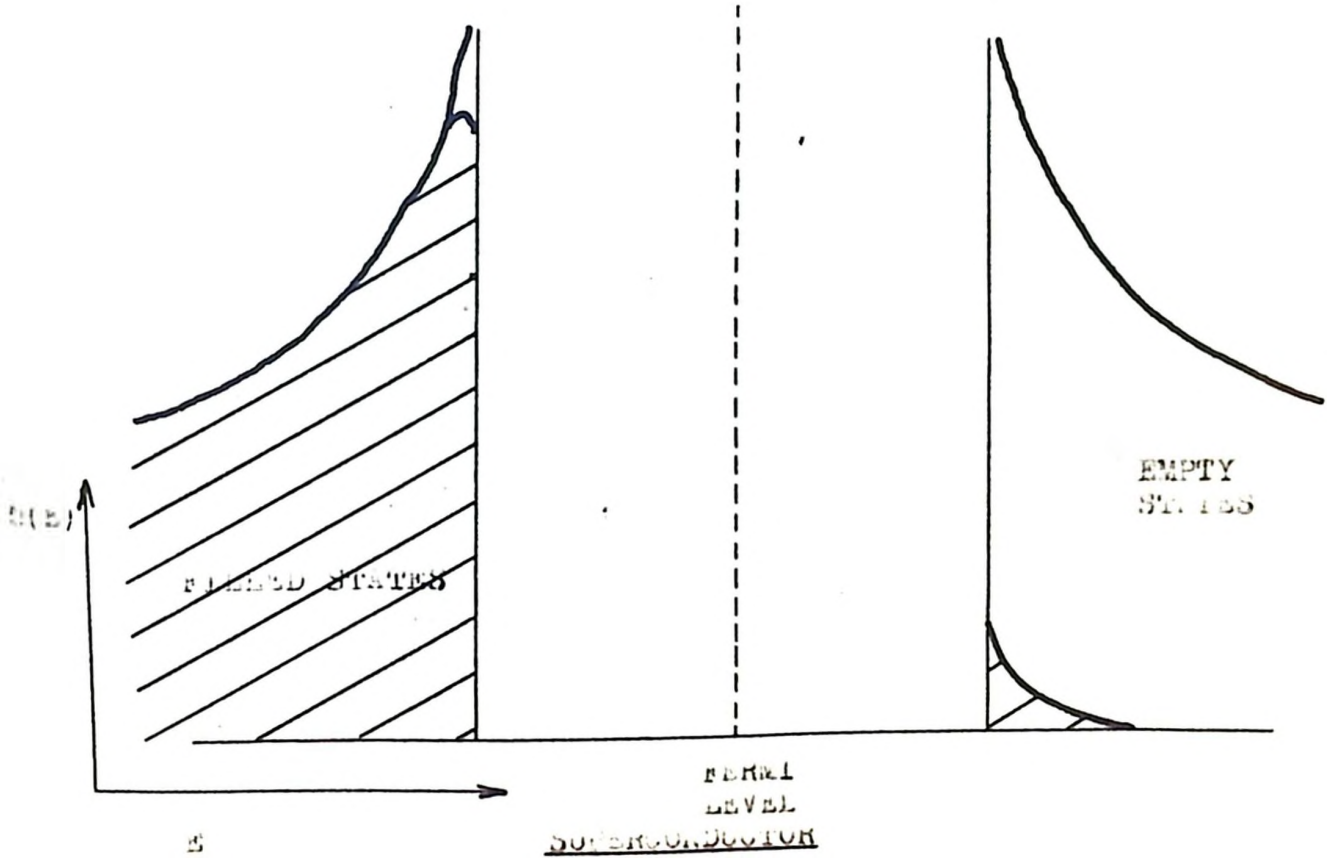

SUPERCONDUCTOR

curve with this infinitely sharp probe which has far more available energy states, than a normal metal at the Fermi level.

It should be noted, however, that using a probe that is displaced on energy Δ_o below the Fermi level necessitates applying a potential equivalent to

$$\Delta_o + \Delta + \hbar\omega_q$$

to observe the phonon effects previously mentioned.

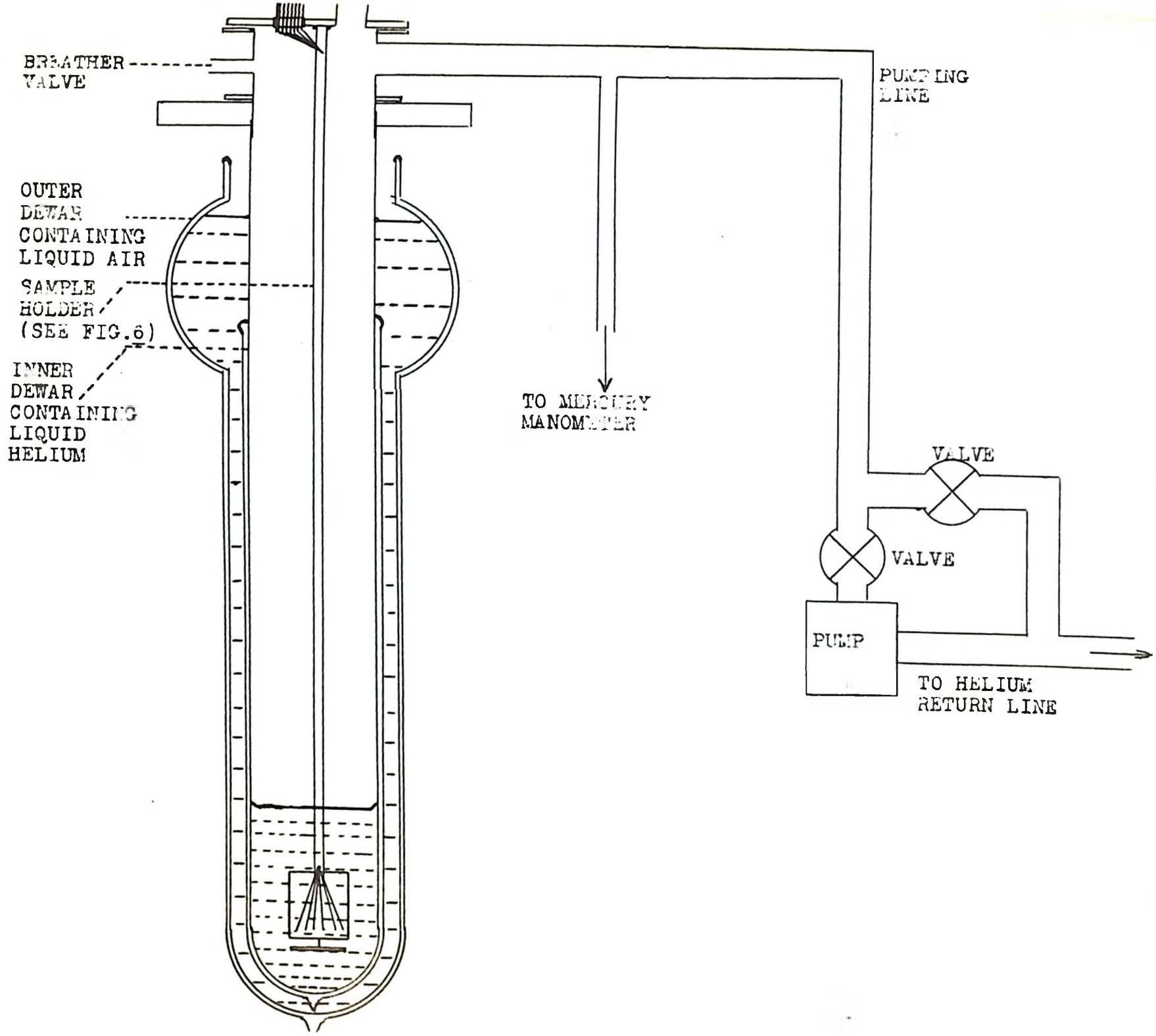
BREATHER VALVE
OUTER DEWAR CONTAINING LIQUID AIR
SAMPLE HOLDER (SEE FIG.6)
INNER DEWAR CONTAINING LIQUID HELIUM
TO MERCURY MANOMETER
PUMPING LINE
VALVE
VALVE
PUMP
TO HELIUM RETURN LINE

III. APPARATUS AND TECHNIQUE

3.1 Cryostat

The cryostat used is as shown in figure 5. This cryostat allows the immersion of the sample under study directly into liquid helium. The system is arranged in such a way that the helium is recovered after the experiment. Connected to the cryostat by means of a 3/4" pumping line is a Welch model 1402 duo-seal vacuum pump with a speed of 140 litres per minute. With this pump it is possible to reduce the temperature of the helium system to 2.0°K. This temperature is quite low enough to study the superconducting properties of lead, which has a transition temperature of 7.2°K.

The holder upon which the sample is mounted is shown in figure 6. This consists of thin-wall stainless steel tubing 1/8 inch in diameter, the top end of which is soldered to the removable part of the head of the cryostat, and the bottom end connected, by means of small bolts, to a piece of non-conducting thin board. It is here that the sample under study is mounted. In the head is mounted a 3/4" kovar seal with eight electrical feed through leads and a tube into which the liquid helium transfer tube can fit. The electrical leads to the sample enter the system through the kovar seal and are connected, through number 38 insulated copper wires to posts on the board at the bottom of the stainless steel rod. These leads go down the cryostat inside the tubing. In addition to the six leads to the sample, there are two more leads which are connected to a heater on the under side of

FIGURE 5

SAMPLE HOLDER

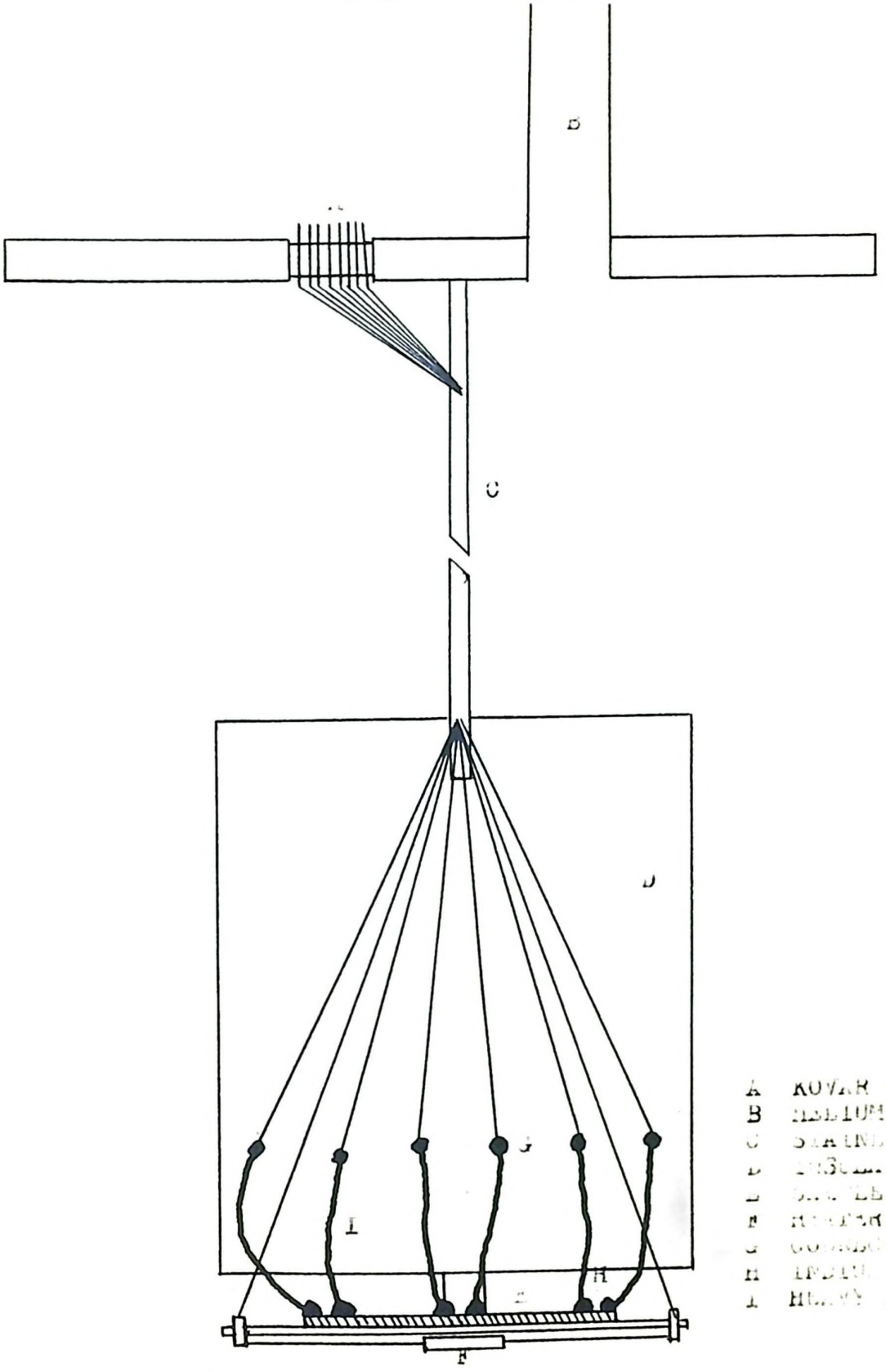

A KOVAR SEAL
B HELIUM [illegible]
C STAINLESS STEEL TUBE
D [illegible]
E [illegible]
F [illegible]
G [illegible]
H [illegible]
I [illegible]

the sample holder proper. This heater consists of four - 47 ohm Allen-Bradley ½-watt resistors in parallel. This heater will boil off approximately one litre of helium an hour under a dissipation of 1 watt.

The temperature of the liquid helium bath may be determined from surface vapour pressure measurements. Sufficiently accurate temperature measurements in this system are made with the aid of a standard mercury manometer.

3.2 Preparation of Superconductive Tunnelling Samples

A suitable tunnelling sample was obtained by deposition of metal films onto a substrate of a flame polished microscope slide section approximately an inch square. The slide was initially outgassed in a vacuum oven for several hours at a temperature of 150°C and a pressure of about 10 microns of mercury. The slide was then cleaned with Ajax cleaner and hot water, and thoroughly rinsed with distilled water, making certain that there was no residual grease or dirt. It was then dried using a tissue designed for use with optical surfaces. Immediately after drying the slide was transferred to a vacuum coating unit. This unit was an Edwards multi-filament coating unit model number 12E3 capable of achieving a vacuum of at least 10^{-6} torr.

The material under study was evaporated from a molybdenum boat through which 30-35 amperes at 3-4 volts was passed. The evaporation occurred in 15-20 seconds.

The glass slide was placed in a slide holder 12" above the filament from which the evaporation was to take place. In front of this slide holder one can place masks which allow strips of different

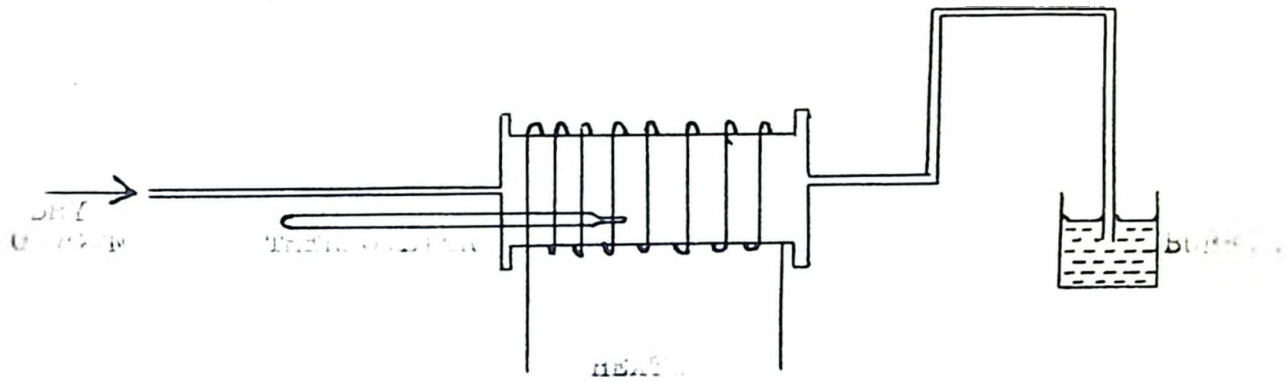

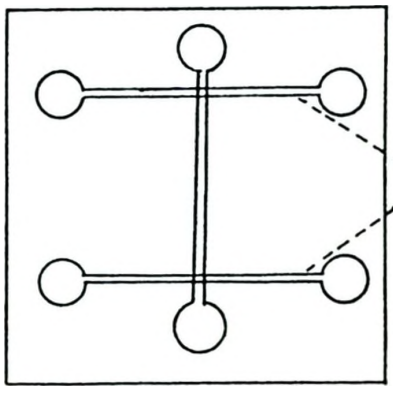

geometries to be deposited. The evaporated film strips were dumbbell shaped, by virtue of the mask design, to facilitate the attachment of electrical leads. Further, as an experimental aid, those masks were so designed to enable two samples to be prepared on the same substrate. The actual metal films were made to be about 1000 to 2000 A° thick and about 0.050" wide. This relatively small width decreased the probability of a hole or short being produced in the oxide, simply because the surface area of the sample was small.

After evaporation of the first metal, the slide was placed in an oxidation chamber (see figure 7a), which was continually flushed with dry oxygen. With this technique a suitable insulating oxide film of thickness required for tunnelling observations could be prepared.

It was observed that the oxidizing parameters were dependent not only on the metal evaporated, but also on the impurity content in the metal. For a pure lead sample (Cominco 99.9999% pure) it was found that it was necessary to place the films in the oxidation chamber for 3 hours at a temperature of 75°C. This amount of oxidation grew an oxide on the surface which gave an ultimate sample tunnelling resistance of 50-100 ohms for the sample geometry employed in these experiments. On the other hand, for a 5% bismuth impurity in pure lead, oxidation for about 2½ hours at 50°C gave approximately the same result. A 10% bismuth impurity required an oxidation time of 2 hours at 45°C to give an oxide of about the same resistance. The thickness of these oxides was not measured directly, but estimated from resistance measurements at room temperature to be about 20 A°.

After this oxidation procedure was completed, the sample was

again placed in the slide holder inside the vacuum coating unit and a film strip of the same material was evaporated onto the substrate at right angles to the oxidized one thus forming 2 small (.05" x .05") junctions of the type metal-insulator-metal (M-I-M). The completed sample was as illustrated in figure 7b.

The sample was then mounted on the insulating board previously described, and electrical leads were connected to it, with the aid of indium solder. It was found that indium made good electrical contact with the films and adhered well, even at liquid helium temperatures. Because of their mechanical fragility the leads were connected to the external circuit via connecting posts mounted on the insulating board

3.3 Preparation of Lead Bismuth Alloys

Tunnelling observations were used as a tool to study the effect of impurities on the density of states of certain superconductors. In particular, it was felt that such studies of Pb-Bi alloys which had been reported by other observers (Al) might yield valuable information on such density of states structures.

These alloys were made in a vacuum of approximately 10^{-5} torr. The constituents of bismuth and lead (5% and 10% bismuth by weight) were placed in a small graphite crucible. This crucible was then placed on a tungsten wire filament and the whole arrangement was mounted inside the Edwards vacuum coating unit. Graphite was chosen because molten lead, when cooled, does not adhere to it. The crucible was heated up to about 350°C until both constituents were in the molten state and allowed to remain in this state for well over 1 hour, with occasional shaking to insure homogeneity. Tunnelling results obtained from material extracted

from different regions of the resulting ingot showed that, within experimental error, the alloy was indeed homogeneous. The crucible and alloy were then quenched in an atmosphere of pure helium gas. It was found that such quenching greatly reduced the amount of oxide formed on the surface.

After the alloy was formed, it was handled exactly as the pure metal. During evaporation, care was taken that all the charge placed in the molybdenum boat was evaporated, in order to insure a correct percentage of the constituents in the deposited film. Also, in order to be certain that the percentage of bismuth in the lead was indeed that prescribed, it was necessary to consider relative evaporation rates. For a pure material Kubaschewski and Evans (K1) show that the evaporation rate of a molten material is given by

$$W = p_o \sqrt{\frac{M}{2\pi RT}} .$$

where p_o = vapour pressure of that material

M = molecular wt. of that material.

For an alloy, it is possible to describe the rate of evaporation of a constituent, say material a

$$W_a = p_a \sqrt{\frac{M_a}{2\pi RT}}$$

where p_a = vapour pressure of the a material above a solution with another material b. This is more often defined in terms of the activity a_a where,

$$a_a = \frac{p_a}{p_o} .$$

In the ideal solution, the vapour pressure of the material is lowered

proportionally to its molar concentration in the mixture. Its activity is therefore, ideally equal to its molar fraction

$$a_a = \frac{p_a}{p_o} = N_a$$

This is just a formulation of Raoult's law. Hence we can write, for bismuth in lead

$$W_{bi} = p_{bi} \sqrt{\frac{M_{bi}}{2\pi RT}} = a_{bi}\, p_{obi} \sqrt{\frac{M_{bi}}{2\pi RT}}$$

Similarly, for the lead in bismuth we can write

$$W_{pb} = p_{pb} \sqrt{\frac{M_{pb}}{2\pi RT}} = a_{pb}\, p_{opb} \sqrt{\frac{M_{pb}}{2\pi RT}}$$

The difference between p_{opb} and p_{obi} is at the most about 10% of the total value (R2) at these temperatures considered, and the deviation from Raoult's law is of the order of a few per cent. Consequently we can be certain that the error in our mixture concentration is not more than ± 1% even for 10% bismuth in lead mixtures. Also, from the repeatability of tunnelling observations made on samples evaporated from different sections of the alloy ingot, we conclude that the alloy is indeed homogeneous and that the above estimates are indeed valid.

3.4 Mercury Sample Preparation

Tunnelling studies on thin mercury films have been reported in the literature (B3). No tunnelling studies on bulk mercury - a strong coupled superconductor - have been reported to date and it was felt that an attempt should be made to study the density of states structure and possible anisotropy in such bulk material. In this respect, attempts

were made to construct a sample incorporating bulk mercury. Samples were prepared of the type Al-Al_2O_3-Hg - aluminium being chosen for its rapidity of oxidation to suitable tunnelling thicknesses, and for the durability of its oxide in tunnelling fabrications at liquid helium temperatures. Because of the obvious difficulty in handling mercury at room temperature, the following fabrication technique was employed. An aluminium film was deposited by techniques previously described, and allowed to oxidize. This oxidation involved simply exposing the film to air for a few minutes. A small tray, through which electrical leads were connected, was then placed on top of the glass slide and the mercury was poured into this tray. As before, the whole system was then mounted on the sample holder and cooled to liquid helium temperatures.

TOP VIEW SIDE VIEW

FIGURE 8
MERCURY TRAY

Unfortunately, with this technique, it was found that the mercury attacked the oxide film, and eventually the aluminium itself, lifting it up from the glass slide. Another method was attempted in which the substrate and aluminium strip were cooled down to 77°K, prior to the pouring of the liquid mercury, in the hope that the aluminium oxide would not be attacked as severely by the mercury. It was found, in all cases, however, that either an extremely high tunnelling resistance or zero resistance resulted.

The former result could possibly be due to the fact that the glass, being at 77°K allowed vapours to condense upon it, thus forming a very thick insulating barrier between the aluminium and the mercury. The latter result was attributed to the penetration of the aluminium oxide by the mercury, as observed with the first mentioned technique.

Because of the inherent limitations of the particular electronic instrumentation employed, satisfactory tunnelling observations could not be made on very high resistance samples. Nor could such observations be made on shorted samples in which the tunnelling current was completely masked by conventional conduction currents.

For these reasons therefore, an investigation of tunnelling in bulk mercury was abandoned in favour of further experiments on lead bismuth alloys.

3.5 Current vs. Voltage Measurements

The circuit used to study the straightforward I-V characteristics of various tunnelling junctions is as shown in figure 9. D-C bias for the junctions is obtained from a Harrison type 6200 A programmable power supply. In this case the output voltage is programmed by a variable external resistor included in the reference feed-back circuit of the supply. For these experiments in particular, a suitable voltage-time sweep was obtained with the aid of a 10-turn, 10000 ohm helipot resistor, driven by either a 1 r.p.m. or 10 r.p.m. reversible a-c motor. For a given motor speed, further control of the bias sweep voltage applied to the sample could be achieved by adjustment of resistance R_L in the power supply output circuit. A typical sweep speed used in this experiment was 1 millivolt per minute.

FIGURE 9

I-V MEASURING CIRCUIT

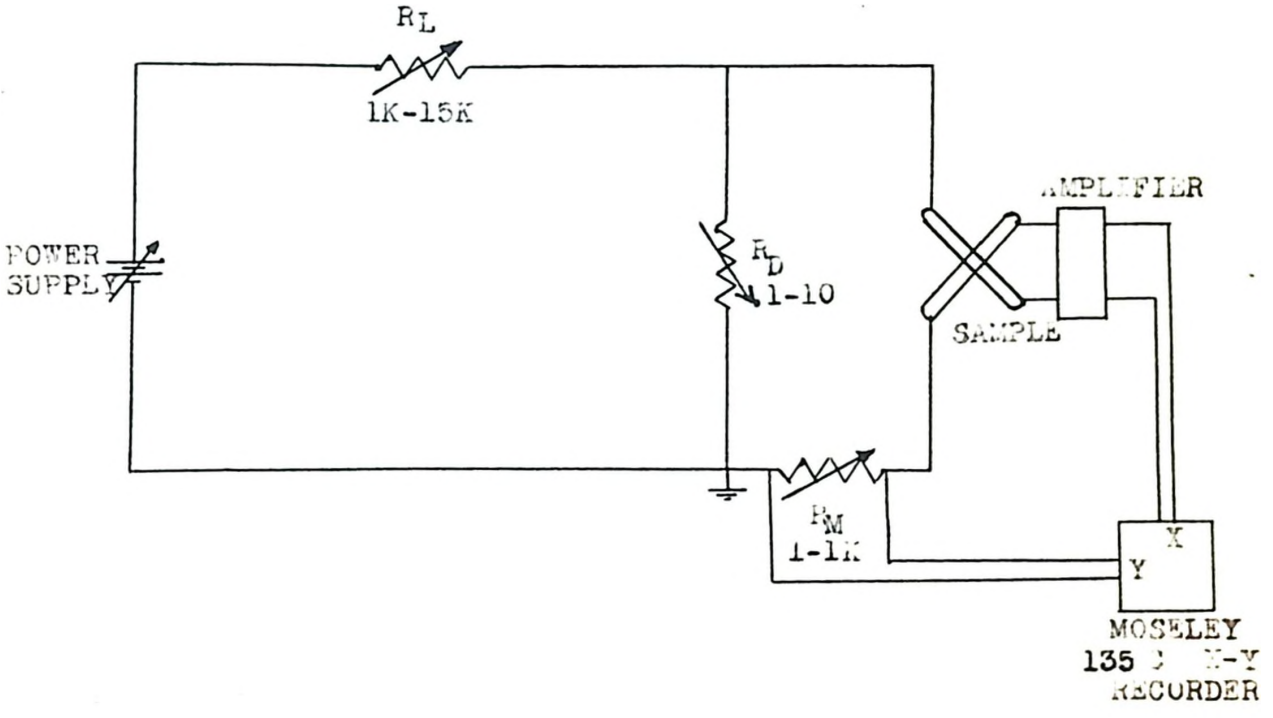

The source impedance as seen by the tunnelling junction is essentially R_D which is always kept much less than the static resistance R_T of the tunnelling sample. This ensures that the tunnelling junction always sees a "constant voltage" source, which is necessary for suitable plotting of the I-V characteristics. Note that this result is only strictly valid when the value of the current measuring resistance R_M is such that $R_D < R_M < R_T$.

To eliminate errors in voltage measurement, the voltage developed across the insulating barrier is measured from the two terminals of the four terminal sample not included in the main current path. This measured voltage is then fed through a Dymec model 2460 A amplifier to the X-input of a Moseley 135C X-Y recorder. This amplifier, with an input impedance of 150 KΩ serves to amplify the tunnel voltage to a suitable level for recording and at the same time eliminates circuit problems associated with the relatively low input impedance of the X-Y recorder on the particular ranges used. As mentioned above, tunnelling currents are obtained from measurements of the voltage drop across the current measuring resistor R_M. This resistor is a selected standard resistor accurate to $\pm$ 1%. This d-c signal across R_M is fed into the Y input of the X-Y recorder. In this current monitoring circuit, impedance levels are such that an intermediate buffer amplifier is not required.

3.6 Derivatives of the I-V Characteristic

As was pointed out in chapter II, for studies of the density of states function both in the region of the energy gap and in the phonon affected region of the superconductor under observation, it is extremely

advantageous to obtain the first $(\frac{dI}{dV})$ and second $(\frac{d^2I}{dV^2})$ derivatives of the current voltage characteristic of a superconducting tunnel junction. A very convenient method of obtaining these functions is with the aid of an a-c modulation technique as will be described below.

If, for a non-linear current-voltage device, one considers the Taylor expansion of current as a function of voltage about an arbitrary reference voltage V_o, one obtains

$$I(V) = I(V_o) + \frac{dI}{dV}\bigg|_{V_o}(V-V_o) + \frac{1}{2!}\frac{d^2I}{dV^2}\bigg|_{V_o}(V-V_o)^2$$

$$+ \frac{1}{3!}\frac{d^3I}{dV^3}\bigg|_{V_o}(V-V_o)^3 + \frac{1}{4!}\frac{d^4I}{dV^4}\bigg|_{V_o}(V-V_o)^4$$

$$+ \text{higher order terms.}$$

If we consider the application of a sinusoidal modulating voltage $V_{ac}\cos\omega t$ causing excursions about the reference voltage such that

$$V-V_o = V_{ac}\cos\omega t\ ,$$

we obtain

$$I(V) - I(V_o) = \frac{dI}{dV}\bigg|_{V_o}(V_{ac}\cos\omega t) + \frac{1}{2!}\frac{d^2I}{dV^2}\bigg|_{V_o}(V_{ac}\cos\omega t)^2$$

$$+ \frac{1}{3!}\frac{d^3I}{dV^3}\bigg|_{V_o}(V_{ac}\cos\omega t)^3 + \frac{1}{4!}\frac{d^4I}{dV^4}\bigg|_{V_o}(V-V_o)^4 + \cdots\cdots$$

After trigonometric expansions for $\cos^2\omega t$, $\cos^3\omega t$ and higher order terms, the above expression may be reduced to

$$I_{ac} = \left(\frac{d^2I}{dV^2}\bigg|_{V_o}\frac{V_{ac}^2}{4} + \frac{d^4I}{dV^4}\bigg|_{V_o}\frac{V_{ac}^4}{4} + \text{higher order terms}\right)$$

$$+ \cos \omega t \left(\frac{dI}{dV}\Big|_{V_o} V_{ac} + \frac{d^3I}{dV^3}\Big|_{V_o} \frac{V_{ac}^3}{8} + \text{higher order terms}\right)$$

$$+ \cos 2\omega t \left(\frac{d^2I}{dV^2}\Big|_{V_o} \frac{V_{ac}^2}{4} + \frac{d^4I}{dV^4}\Big|_{V_o} \frac{V_{ac}^4}{96} + \text{higher order terms}\right)$$

$$+ \cdots\cdots$$

where $I_{ac} = I(V) - I(V_o)$.

The fundamental current component that results from such modulation is therefore

$$I_{ac}(\omega) = \cos \omega t \left(\frac{dI}{dV}\Big|_{V_o} V_{ac} + \frac{d^3I}{dV^3}\Big|_{V_o} \frac{V_{ac}^3}{3} + \cdots\cdots\right).$$

It is found that, considering the parameters used in this experiment, the second and remaining terms contribute less than 1% of the total of this summation. Hence, to a good approximation we obtain

$$I_{ac}(\omega) = \frac{dI}{dV}\Big|_{V_o} V_{ac} \cos \omega t,$$

or $\frac{dI}{dV}\Big|_{V_o} = C_{ac}$ where C_{ac} is the dynamic a-c conductance. Thus, with such a suitable modulation voltage applied to a tunnelling junction the $\frac{dI}{dV}$ function may be easily obtained at a given reference voltage. It is seen that if this reference voltage itself is, in addition, made to be linearly and slowly time varying, then the $\frac{dI}{dV}$ function may be obtained over the entire region of bias interest.

In a similar fashion the first harmonic current component is given by

$$I_{ac}(2\omega) = \cos 2\omega t \left(\frac{d^2I}{dV^2}\Big|_{V_o} \frac{V_{ac}^2}{4} + \frac{d^4I}{dV^4}\Big|_{V_o} \frac{V_{ac}^4}{96} + \cdots\cdots\right).$$

Again it is valid to within 1% to truncate the series after the first term and we obtain

$$I_{ac}\ (2\omega) = \cos 2\ \omega t \left.\frac{d^2I}{dV^2}\right|_{V_o} \frac{V_{ac}^{\ 2}}{4}$$

$$\text{or } \left.\frac{d^2I}{dV^2}\right|_{V_o} = \frac{4\ I_{ac}\ (2\omega)}{V_{ac}^{\ 2} \cos 2\ \omega t}$$

Consequently, by measuring the first harmonic component of the current produced through the sample, we can obtain $\frac{d^2I}{dV^2}$ directly over the region of bias interest.

The circuit used to achieve this end is as illustrated in figure 10. The oscillator used supplies a 1000 c.p.s. signal with a relatively small amount of distortion from a pure sine wave. Because it is of a high enough frequency that it will not be affected by the d-c sweep, and because of the practical convenience of it, a 1000 c.p.s. frequency was used. In order that all harmonics produced in the circuit are a result of the non-linearity of the device under study, it is imperative that no 2000 c.p.s. component be coming from this oscillator. For this reason, two - 1000 c.p.s. low pass filters are connected directly to the output of this instrument. With these filters, the 2000 c.p.s. component is less than .2% of the original signal. This modulation is inserted into the circuit across R_D so that the small modulation will be seen by the sample on top of the larger d-c sweep voltage. The amplitude of this modulation must be small as compared to the detail on the curve which is to be investigated. If the modulation is of the same order as the detail, the modulating signal will gloss over the sharpness and thus cause a type of smearing.

FIGURE 10

DIFFERENTIATING CIRCUIT

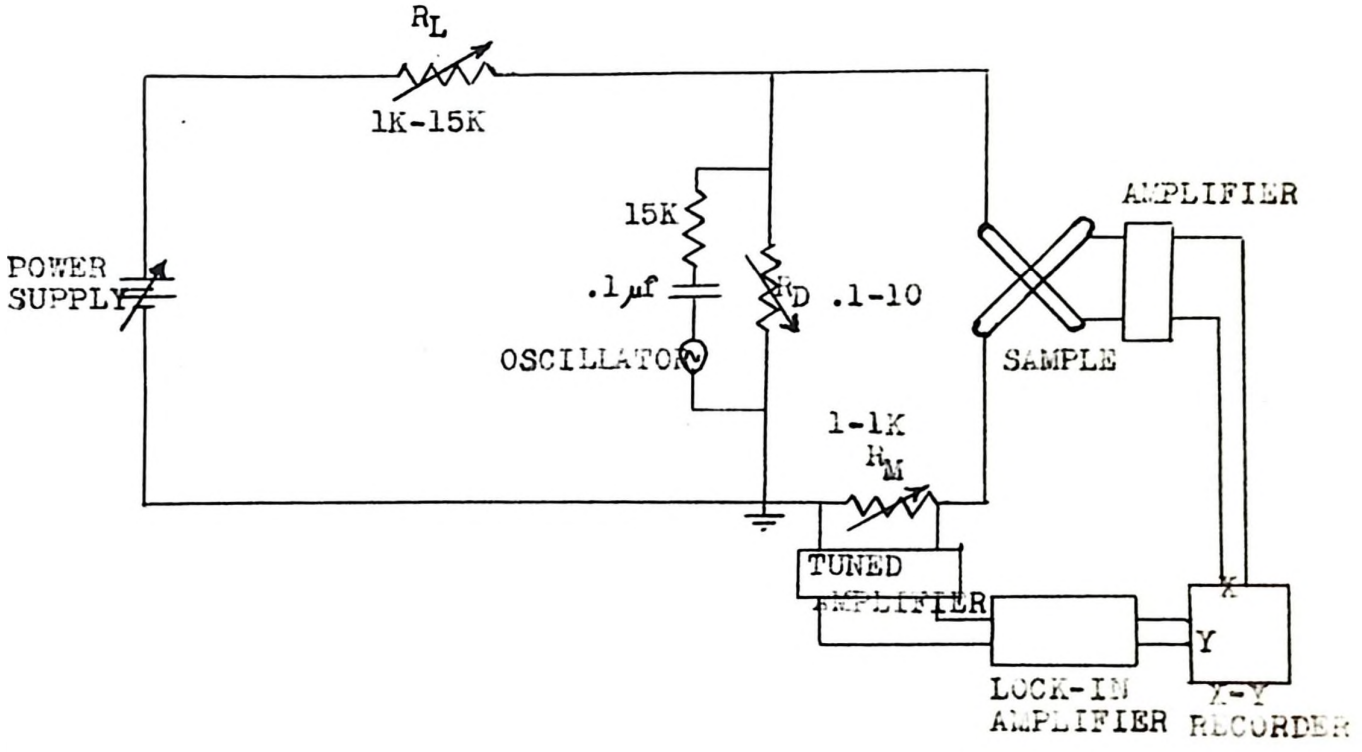

Also, if the d-c sweep is fast or jerky and of the same rate as the modulating signal sweep, the harmonics of 1000 c.p.s. produced will not be a true indication of the non-linearity of the tunnelling junction but will also be a function of the sweep speed. In order to eliminate this problem, the d-c sweep must be very slow. A typical sweep speed used in this experiment is 1 millivolt per minute. This sweep does not in any visible way affect the resultant harmonics of the modulating signal.

For measurements in the region of the energy gap an a-c probe of 50 to 75 microvolts peak to peak seemed adequate to determine the derivatives of the curve without appreciable smearing. In regions of energy far above that of the energy gap, it was found that, due to the fact that the alteration of the density of states curve by interactions with the phonons of the metal was small, the harmonic of such a signal was extremely difficult to detect. Hence it was necessary to increase the a-c modulation level in this region in order to detect any harmonic of the fundamental signal and hence any second derivative. Increasing the modulation to approximately 350 microvolts peak to peak seemed to give an appreciable signal with very little apparent smearing. Even after this increase in signal it was found that the resultant harmonic was of the order of .1 microvolt at the points of largest signal in the phonon affected region of the curve. Consequently, the major problem confronting this method of finding derivatives is that of suppressing the noise and allowing the pure signal to be filtered through. Across the current measuring resistor $R_{..1}$ (from which we measure I_{ac}) there is a General Radio tuned amplifier model 1232-A tuned to the desired

frequency (either 1000 c.p.s. for $\frac{dI}{dV}$ or 2000 c.p.s. for $\frac{d^2I}{dV^2}$). This instrument has a band width of 5% of the tuned frequency and is capable of an amplification of 10^6. From this instrument the amplified signal is fed into a Princeton Applied Research model JB-4 lock-in amplifier which filters, amplifies and detects a desired frequency, giving a d-c output proportional to the signal at that frequency. From this detector the d-c signal is fed into the Y input of an X-Y recorder thus giving us the desired derivative as a function of applied voltage V. By adjusting the output filter on the lock-in amplifier and varying the sweep speed of the power supply accordingly, much of the pick-up noise is reduced without appreciably altering the resolution of the apparatus.

It is also necessary to supply to this lock-in amplifier a reference signal which has the same frequency as, and is at a fixed phase to the signal under observation. This is achieved by means of the following circuit:

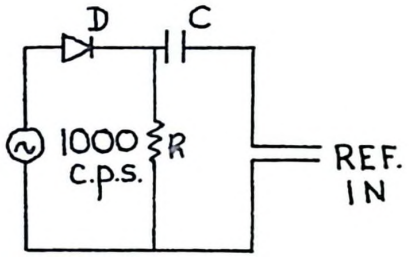

The diode is inserted to give a substantial harmonic to the fundamental signal so that both 1000 c.p.s. and 2000 c.p.s. signals are fed into the reference input.

FIGURE 11

I-V CHARACTERISTIC FOR Pb-I-Pb

T=2.0°K

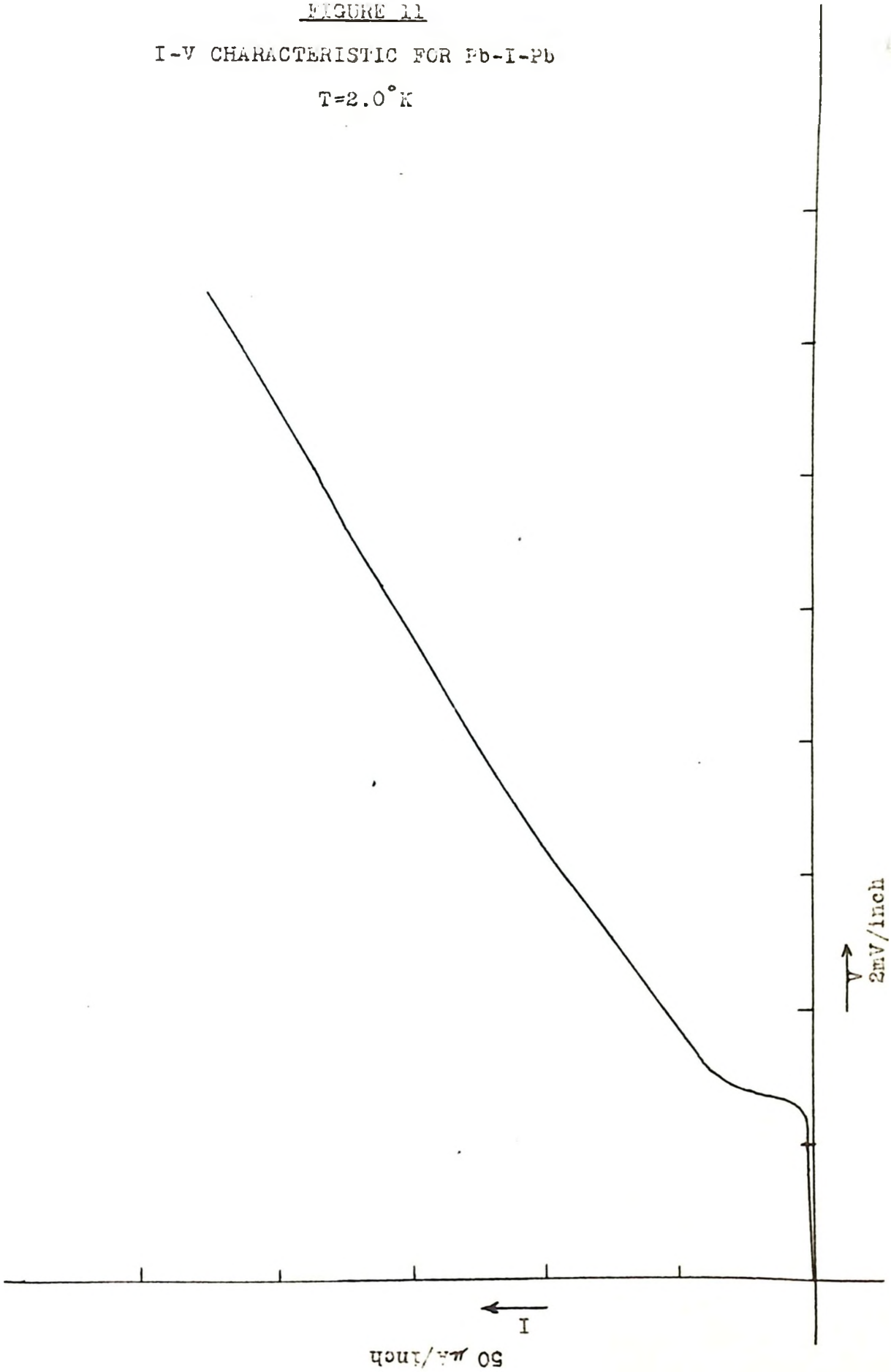

IV. RESULTS AND DISCUSSION

4.1 Superconductor Energy Gap Characteristics

As was discussed in chapter II, a particularly convenient method of determining the width of the energy gap is by measurement of the I-V characteristic curve with both metals in the superconducting state. An even more accurate value is achieved when the superconducting metals are similar. In general, for two similar superconductors and operating temperatures well below the critical temperature, we would expect to see almost zero current until the point 2Δ is reached at which point a sharp rise in the current should result.

Figure 11 shows an experimental plot of current vs. voltage for a lead-insulator-lead junction measured at $2.00^{\circ}K$, with the applied voltage V extending from 0 to approximately 15 millivolts. The uncertainty of the curve is within the thickness of the recorder trace. This I-V curve exhibits this expected almost negligible current flow until the voltage corresponding to the energy 2Δ is applied. At this point, however, there is a slight disagreement with the BCS theory which predicts a discontinuous rise. Since there is no discontinuous jump at this point, a certain amount of ambiguity is introduced in selecting the voltage corresponding to 2Δ. It is assumed that the point at which the slope of the I-V characteristic passes through a maximum indicates the energy gap 2Δ. Effectively, this corresponds to the point where, for an incremental change in voltage ΔV, there are a maximum number of available states into which tunnelling can occur.

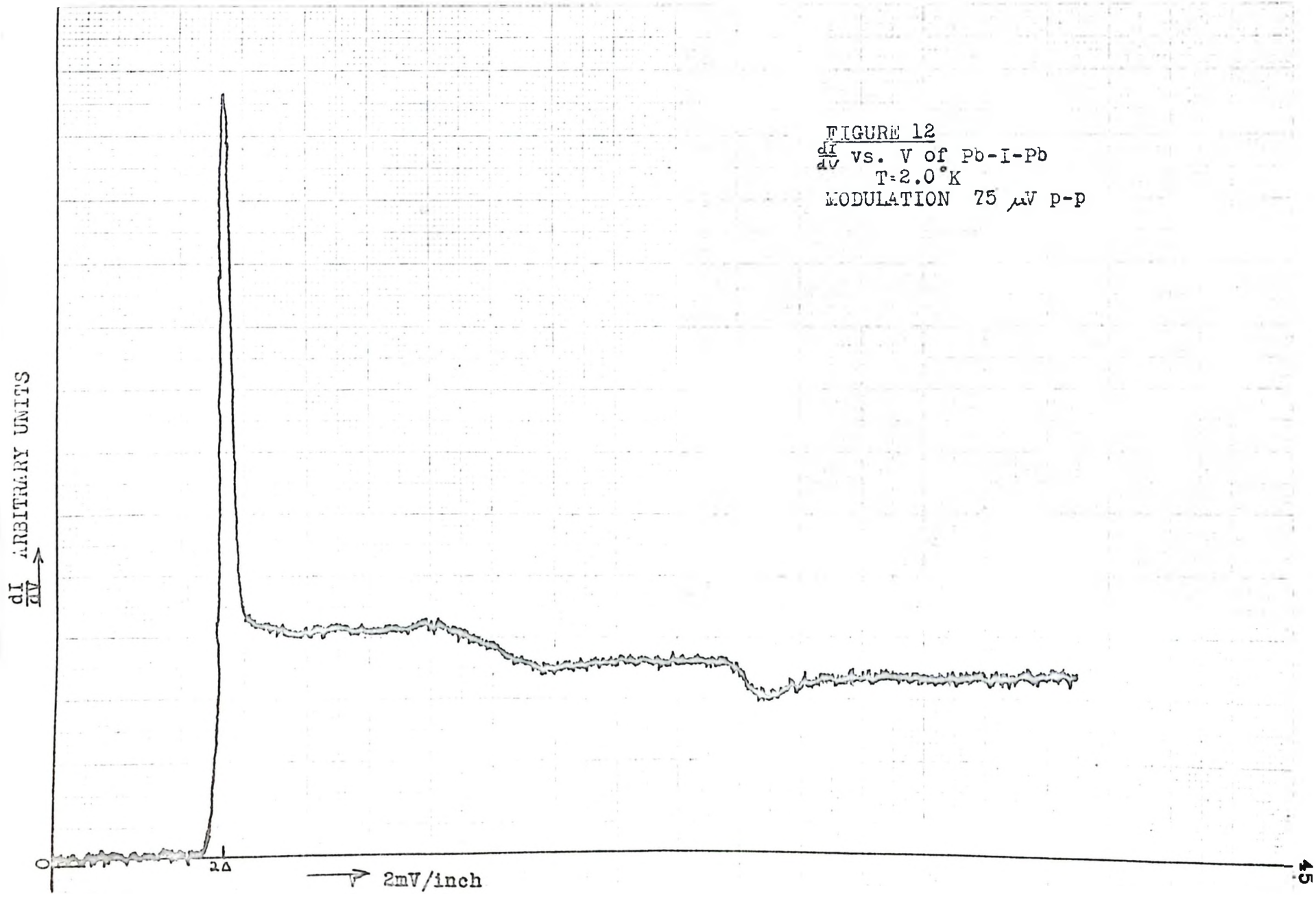

FIGURE 12
$\frac{dI}{dV}$ vs. V of Pb-I-Pb
T=2.0°K
MODULATION 75 μV p-p

Consequently, it seems obvious that a plot of $\frac{dI}{dV}$ vs. V would be a more helpful aid in determining the value of the energy gap. A plot of this function is illustrated in figure 12 and at a glance one can readily see that the point of maximum slope is very easy to discern.

Using this criterion, we conclude that the energy gap as measured for thin lead films at 2.0°K is $2\Delta = 2.70 \pm .05 \times 10^{-3}$ eV

$$\text{or } \Delta = 1.35 \pm .025 \times 10^{-3} \text{ eV.}$$

Using the relation (L3)

$$\Delta(T) = \Delta(0) \left[1 - \left(\frac{T}{T_c}\right)^4 \right]^{-\frac{1}{2}}$$

where $\Delta(0)$ = energy gap at 0°K and the bulk critical temperature $T_c = 7.18$°K for lead, we calculate that

$$\Delta(0) = 1.35 \pm .025 \times 10^{-3} \text{ eV}$$

which, expressed in terms of kT_c is

$$2\Delta(0) = 4.35\ kT_c.$$

This value is in good agreement with that given by Giaever and Megerle (G4) using tunnelling techniques and by Ginsberg and Tinkham (G5) from infrared transmission. It should also be noted that this is not in particularly good agreement with the BCS weak coupling model which gives (equation 20)

$$2\Delta(0) = 3.52\ kT_c.$$

Of considerable interest is this smearing around the gap edge or the non-discontinuous jump. This smearing could be due to, among other things: 1) non-uniform strain set up in the film due to the

unequal contraction of the substrate and the film, 2) anisotropy of the energy gap. It has been suggested (T2) that a variation in the energy gap over the Fermi surface should be observed. Anderson (A3) claims that if the collision time for scattering of electrons against impurities is short enough so that the mean free path, $\ell \lesssim \xi_o$, (the coherence distance) the rapid scattering will connect states all around the Fermi surface producing a sharp "isotropic" gap. Comparison of figure 13 with figure 11 which is a similar I-V plot of lead-insulator lead with a 5% bismuth impurity in the lead ($\ell \approx \xi_o$), will immediately indicate that the sharpness of the rise is much more marked with a small amount of impurity present. These results seem to indicate that the smearing in the pure material is perhaps due to a small anisotropy of the lead energy gap.

4.2 Density of States

According to theory, the quantity most closely related to the superconducting tunnelling density of states is the first derivative of the current voltage characteristic. At $T = 0^oK$, $\frac{dI}{dV}$ should be directly proportional to the density of states, while for temperatures greater than this, $\frac{dI}{dV}$ and N(E) are related by equation 24. Figure 12 is a plot of $\frac{dI}{dV}$ vs. V obtained with the first derivative circuit as applied to a lead-insulator-lead system. The maximum a-c modulation is 75 μV peak to peak. It should be noted that this curve approximates the theoretical BCS density of states function as given in figure 2, except that a displacement of Δ in energy is inherent because the probe used to study the density of states curve is removed from the Fermi surface by a distance Δ. The observed smearing of the first derivative

FIGURE 13

I-V CHARACTERISTIC of $(Pb_{95}Bi_5)$-I-$(Pb_{95}Bi_5)$
T=3.0°K

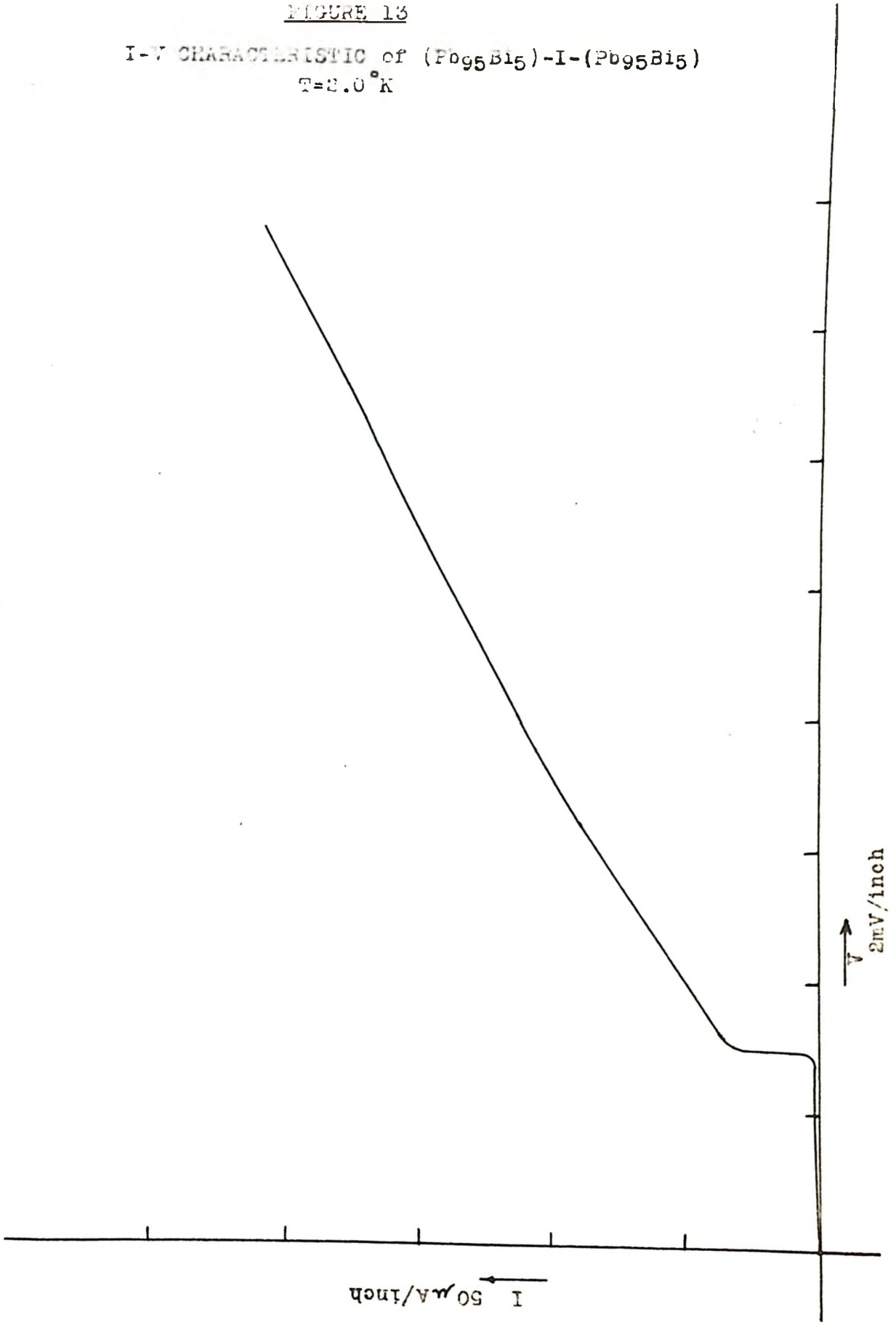

characteristic about the energy gap edge can be attributed both to the finite size of the modulation signal and to anisotropy of the energy gap itself.

As was explained in chapter II, one should expect to observe distinctive structure in the superconducting tunnelling density of states which can be related to the phonon spectrum of that material. Peaks in the phonon spectrum at energies $\hbar\omega_q$ produce drops in the density of states at energies equal to $\hbar\omega_q + \Delta$ above the Fermi level, or $\hbar\omega_q + 2\Delta$ in the type of plot illustrated in figure 12. In figure 12 we see that, at regions well above that of the energy gap, there is distinct and undeniable structure. The drops in $\frac{dI}{dV}$ at energies of approximately 7 and 11 mV's are unmistakable. In fact, even very close scrutiny of the original I-V characteristic (figure 11) shows some non-linear detail in this region.

A particularly useful and sensitive method for investigating this structure is to measure the behaviour of the second derivative of the tunnelling current with respect to the voltage (i.e., $\frac{d^2I}{dV^2}$ vs. V). The location of sharp drops in the density of states curve produced by peaks in the phonon distribution can be determined by the points of maximum negative slope in the differential conductance $\frac{dI}{dV}$. These points correspond, in the derivative of the differential conductance, (i.e., $\frac{d^2I}{dV^2}$) to negative peaks whose positions are much easier to discern. Moreover, structure very difficult to see in the first derivative should show up quite clearly.

With this end in mind, a plot of $\frac{d^2I}{dV^2}$ vs. V was made (figure 14) and it was found to agree extremely well with results reported by other observers (R3). A detailed method of interpeting these curve in terms

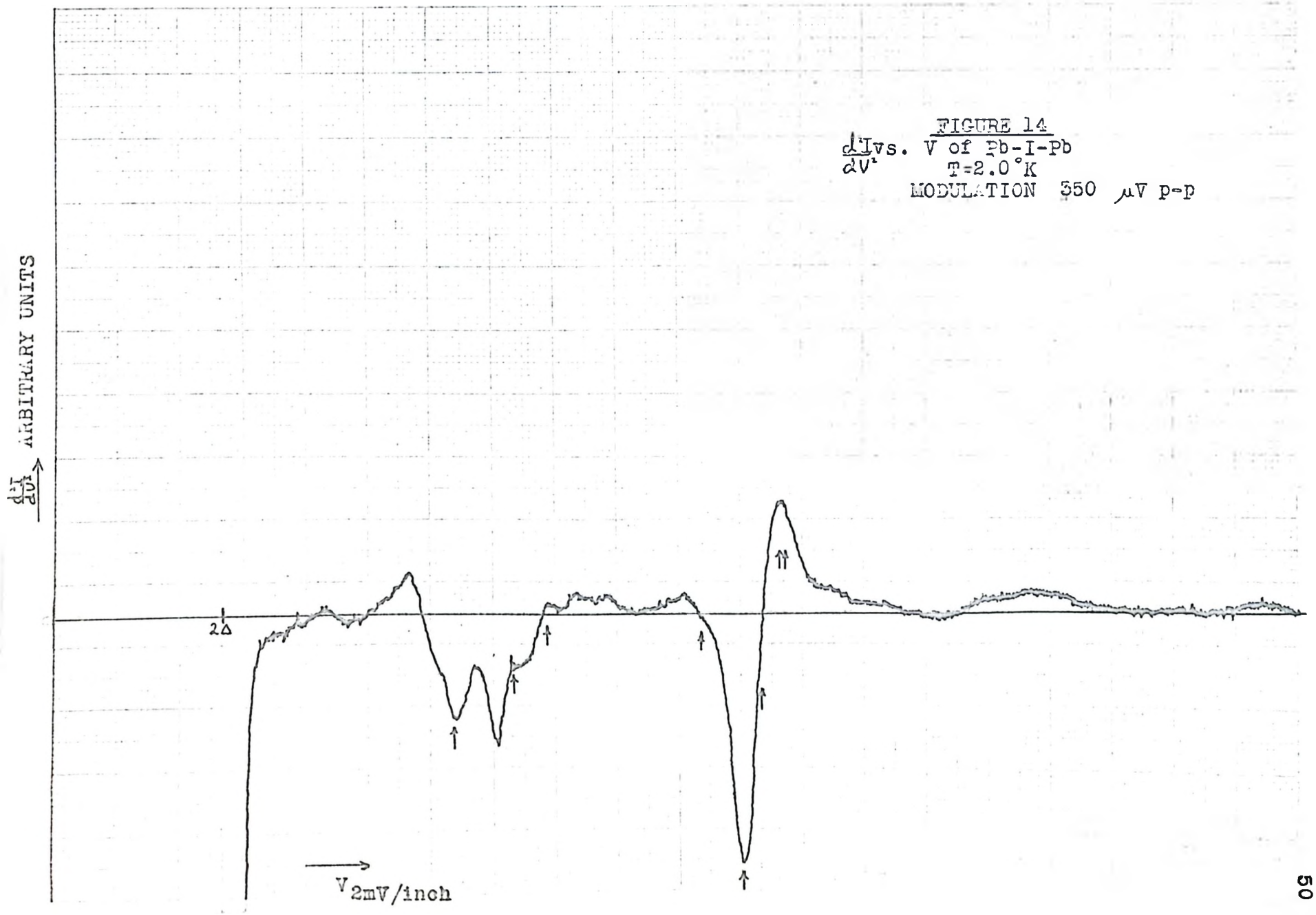
FIGURE 14
d²I/dV² vs. V of Pb-I-Pb
T=2.0°K
MODULATION 350 μV p-p
d²I/dV² ARBITRARY UNITS
2Δ
V 2mV/inch

of electron phonon interactions (R3) and the results of this analysis are in good agreement with those obtained by Brockhouse from neutron scattering data (B4). In this figure, we can identify a set of peaks around 4.5 mV's with transverse phonons and a set at about 8.5 mV's with longitudinal modes. This tunnelling technique of investigating the phonon spectrum of a material has also been extended by other investigators to the study of tin, thallium (R3), mercury (B3) and indium (A2).

4.3 Bismuth Impurities

We have observed that the introduction of 5% and 10% impurities of bismuth into pure lead causes a widening of the energy gap. This widening of the energy gap with impurities is illustrated in figures 15 and 16 from which we derive the following table:

RELATION OF ENERGY GAP WITH %Bi IMPURITY

%Bi in Lead	Energy Gap ($2\Delta(0)$)
0	2.70 ± .05 meV
5	2.95 ± .05 meV
10	3.15 ± .05 meV

This widening of the energy gap with increased bismuth impurity is in agreement with Leslie and Ginsberg (L2) who observed, from far infrared absorption experiments, that as small amounts of bismuth impurity are added to the lead, the energy gap widens. It was suggested that the energy gap is widened because of a net shifting of the phonon spectrum, but at that time no experimental data was available on the spectrum of these alloys. A shift in the average of the phonon energies would

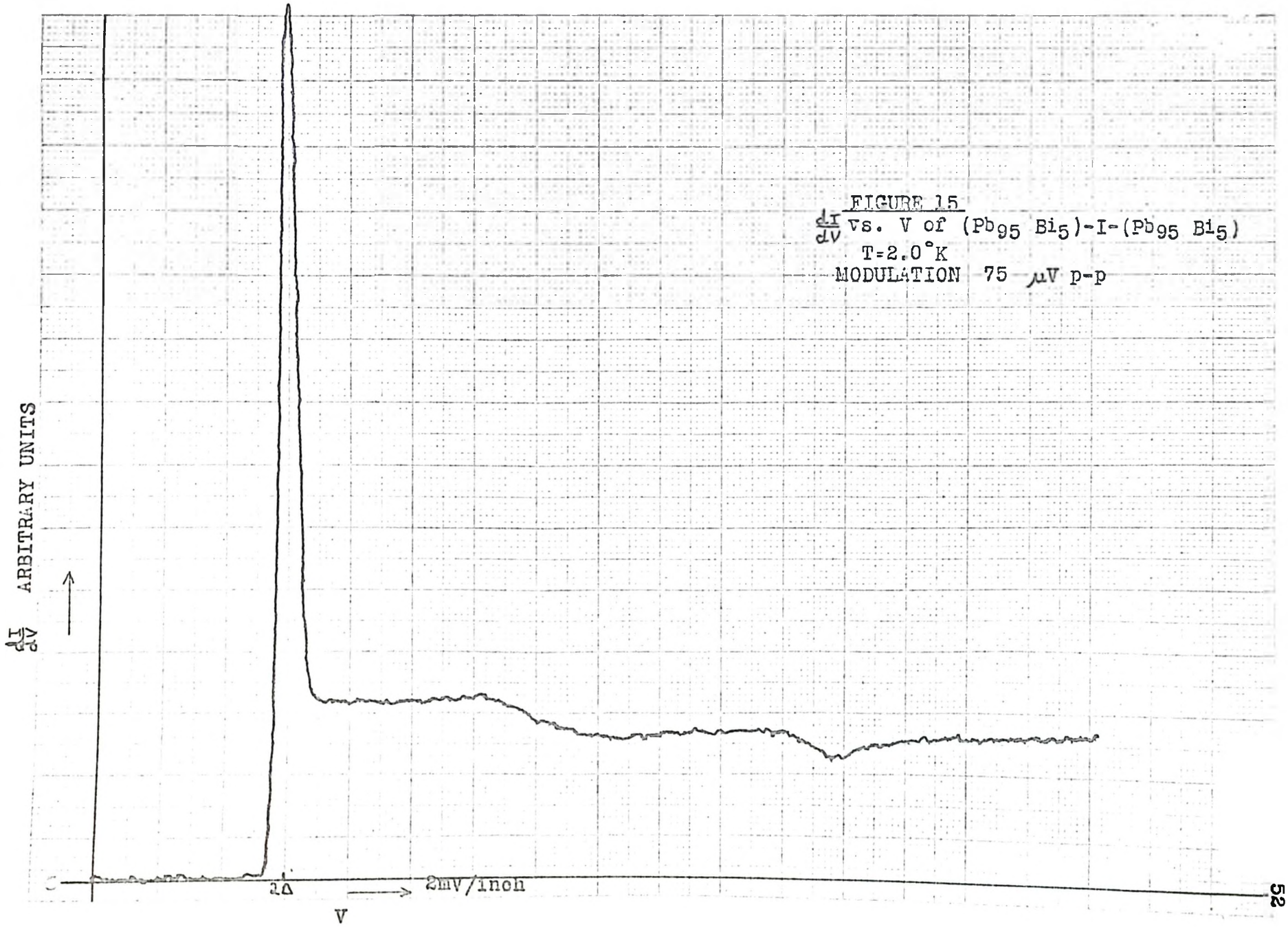

FIGURE 15
$\frac{dI}{dV}$ vs. V of $(Pb_{95}\ Bi_5)$-I-$(Pb_{95}\ Bi_5)$
T=2.0°K
MODULATION 75 μV p-p

FIGURE 16

$\frac{dI}{dV}$ vs. V of $(Pb_{90}\ Bi_{10})$-I-$(Pb_{90}\ Bi_{10})$

T=2.0°K

MODULATION 75 μV p-p

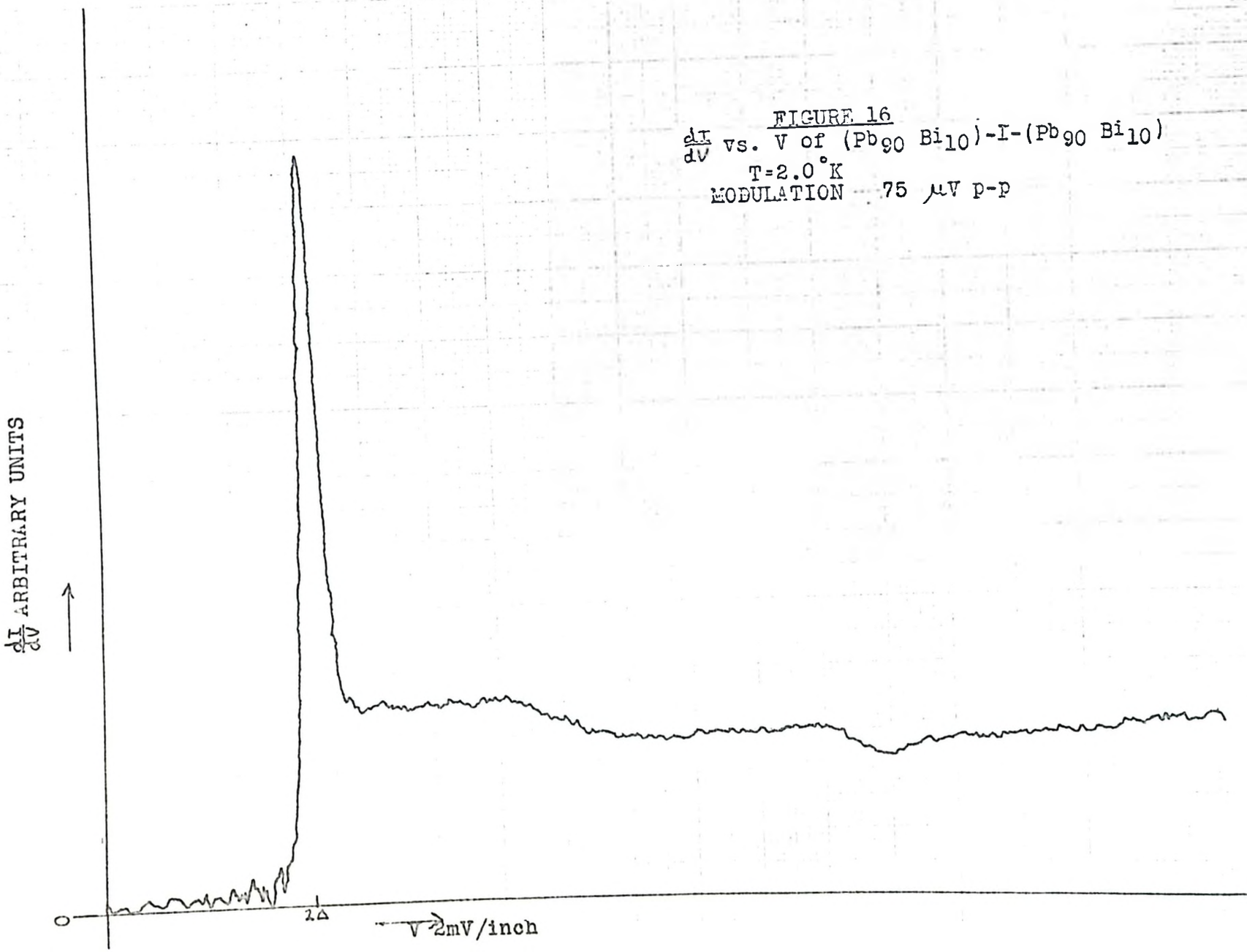

indeed result in a corresponding shift of the size of the energy gap, as can be readily seen from consideration of equation 15, i.e.,

$$\Delta = 2\hbar\omega_q \, e^{-\frac{1}{N(0)V}}$$

where we get an expression of the energy gap dependence on the phonon energies $\hbar\omega_q$.

It should be noted here that these values disagree slightly with those reported by Adler and Mg (Al) using samples of Al-Al_2O_3-Pb with varying degrees of bismuth impurities in the lead. It is felt that using two similar superconductors decreases the ambiguity of measurement by a sizable amount. Also, the criterion used to select the edge of the energy gap is not universally accepted and discrepancies in results with other investigators could be attributed to this.

The second derivative plots of 5% and 10% bismuth impurities are illustrated in figures 17 and 18 respectively. Immediately one can see that the peaks due to the phonon effects are being altered quite markedly. At the points indicated by arrows there is a shift of certain peaks indicating a probable shifting in energy of various peaks in the phonon spectrum. In the longitudinal phonon region case, there seems to be a splitting of the peak around 8.5 mV's into two discernable peaks; the total area under the curve remaining approximately constant. This result seems to indicate that a certain number of the modes are shifting slightly in energy. This shift is of the order of 5% of the total energy and the strength of this peak is quite obviously dependent on the amount of impurity atoms in the material. In other words, the more impurity atoms present in the metal, the more frequent is this new mode.

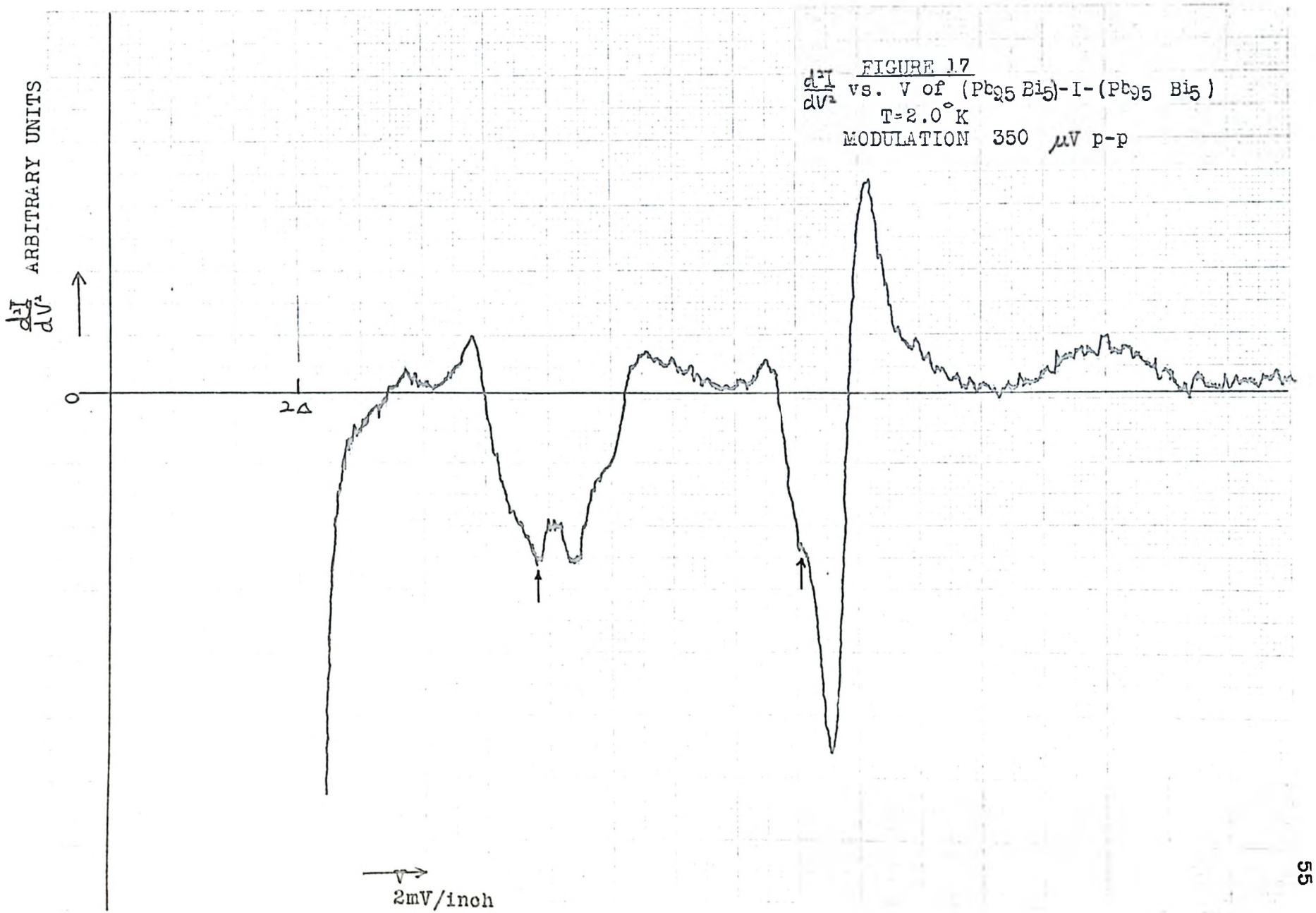

FIGURE 17
$\frac{d^2I}{dV^2}$ vs. V of $(Pb_{95}Bi_5)$-I-$(Pb_{95}Bi_5)$
T=2.0°K
MODULATION 350 μV p-p

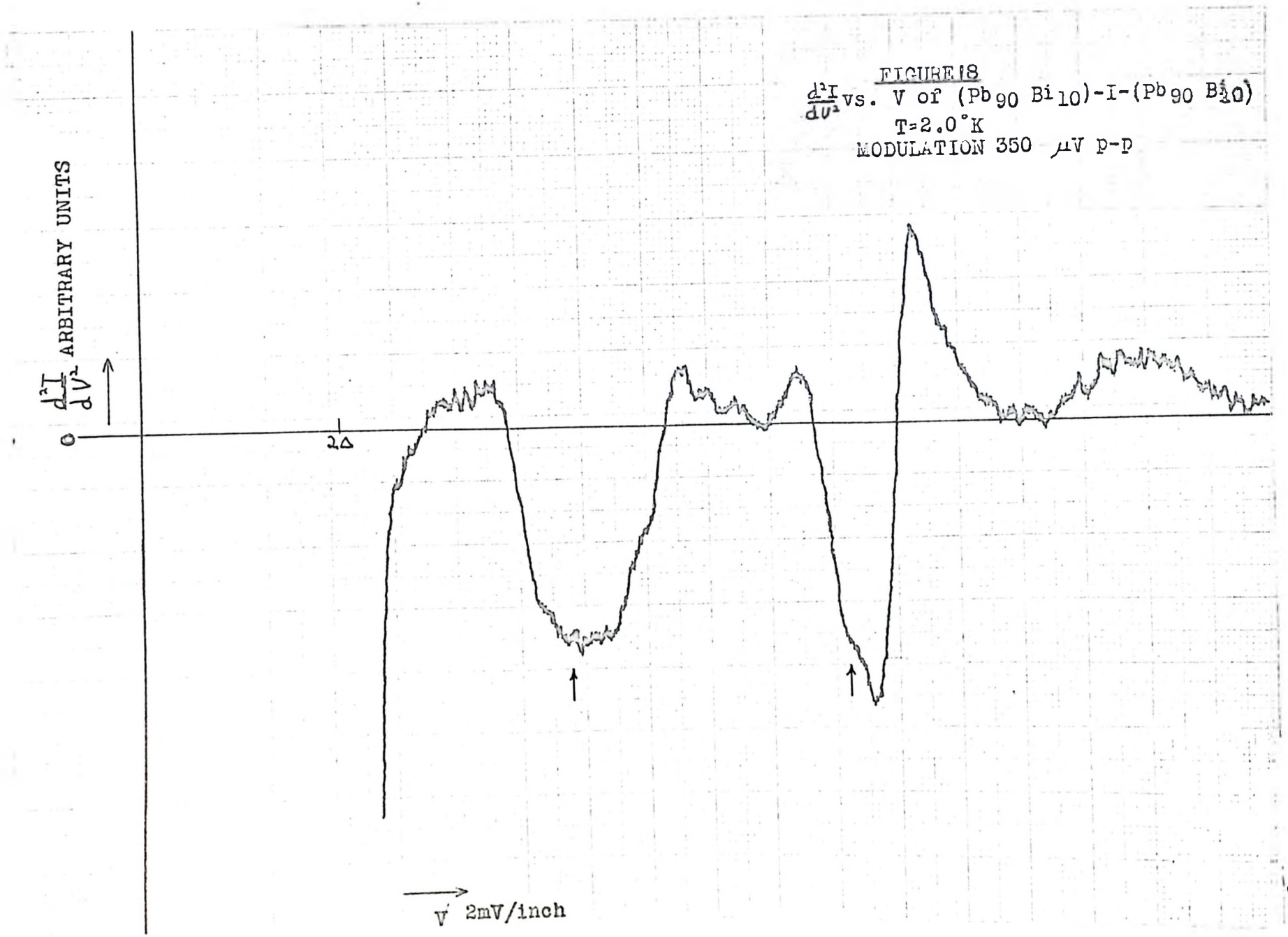
FIGURE 18
$\frac{d^2I}{dV^2}$ vs. V of $(Pb_{90}\ Bi_{10})$-I-$(Pb_{90}\ Bi_{10})$
T=2.0°K
MODULATION 350 μV P-P
$\frac{d^2I}{dV^2}$ ARBITRARY UNITS
0
2Δ
V 2mV/inch

Although it is not quite as obvious, there is a rather large change in the transverse modes about the region of 4.5 mV's. A widening of the basic pattern is evident and a shifting of the two peaks relative to each other both in energy and relative intensity occurs. This is even more spectacular when a 10% bismuth impurity is injected as illustrated in figure 18.

The net effect of all this shifting both in energy and intensity is undoubtedly a resulting shift in the phonon spectrum of the material. As was mentioned above, a net shift in the average energy of the phonons would probably bring about a change in the energy gap of the superconductor.

Unfortunately, no neutron scattering data is available with which one can compare these results. On the strength of the results reported here, however, one can predict, with a certain degree of confidence, that a similar shift in some of the phonon dispersion curves for certain directions will result and that the intensity or frequency of occurrence of these shifts will be a function of concentration of impurity. It is impossible, without inelastic neutron scattering data, to relate these shifting peaks to any explicit modes.

V. CONCLUSIONS AND SUGGESTIONS FOR FURTHER EXPERIMENTS

This tunnelling method of investigation can be applied to almost any superconductor provided temperatures low enough below the critical temperature are available. For weak coupled superconductors, the alteration of the density of states curve caused by the interaction with the phonons is not as great but is still observable using this technique.

This method appears to be a reasonably accurate, rapid, preliminary experiment to the slower and more exacting, neutron diffraction analysis for, in a relatively small amount of time one can, in a qualitative manner, determine what sort of changes in the phonon dispersion curves could be expected with the introduction of impurities. Also, after more quantitative data is available, a relation between the percentage of impurities and the phonon spectrum shift could be more easily determined than with the neutron scattering method.

Another experiment which might prove extremely interesting is that in which impurities of thallium are introduced into lead. Leslie and Ginsberg (L2) have shown by infrared adsorption that, unlike the addition of bismuth, the introduction of thallium causes a narrowing of the energy gap. A study of the probable shift of the phonon spectrum using this technique, would yield valuable information and together with the data obtained with bismuth impurities, one could derive conclusions concerning the interaction of these impurities with the original metal.

BIBLIOGRAPHY

A1 Adler, J. G., Ng, S. C., Can. J. Phys. 43, 594 (1965).

A2 Adler, J. G., Rogers, J. S., Woods, S. B., Can. J. Phys. 43, 557 (1965).

A3 Anderson, P. W., J. Phys. Chem. Solids 11, 26 (1959).

B1 Bardeen, J., Cooper, L. N., Schrieffer, J. R., Phys. Rev. 108, 1175 (1957).

B2 Bardeen, J., Phys. Rev. Letters 9, 147 (1962).

B3 Bermon, S., Phys. Rev. 135, A306 (1964).

B4 Brockhouse, B. N., Arase, T., Caglioti, G., Rao, K. R., Woods, A. D. B., Phys. Rev. 128, 1099 (1962).

C1 Cooper, L. N., Phys. Rev. 104, 1189 (1956).

C2 Chambers, R. G., Proc. Roy. Soc. London A65, 458 (1952).

D1 Deaver, B. S., Fairbank, W. M., Phys. Rev. Letters 7, 43 (1961).

D2 Doll, R., Nabauer, M., Phys. Rev. Letters 7, 51 (1961).

F1 Fröhlich, H., Phys. Rev. 79, 845 (1950).

G1 Gorter, C. J., Casimir, H. B. G., Phys. Z. 35, 963 (1934).

G2 Giaever, I., Phys. Rev. Letters 5, 147 (1960).

G3 Giaever, I., Hart, H. R., Megerle, K., Phys. Rev. 126, 941 (1962).

G4 Giaever, I., Megerle, K., Phys. Rev. 122, 1101 (1961).

G5 Ginsberg, D. M., Tinkham, M., Phys. Rev. 118, 990 (1960).

K1 Kubaschewski, O., Evans, E., Metallurgical Thermochemistry (Macmillan Co., New York, 1958), p. 154.

L1 London, F., London, H., Proc. Roy. Soc. Lond. A149, 71 (1935).

L2 Leslie, J. D., Ginsberg, D. M., Phys. Rev. 133, 362 (1962).

L3 Lynton, E. A., Superconductivity (John Wiley and Sons, Inc., New York, 1962), p. 62.

M1 Meissner, W., Ochsenfeld, R., Naturwiss 21, 787 (1933).

O1 Onnes, H. K., Leiden Comm. 122b, 124c (1911).

P1 Pippard, A. B., Faber, T. E., Progr. Low. Temp. Phys. I, 159 (1955).

R1 Rowell, J. M., Anderson, P. W., Thomas, D. E., Phys. Rev. Letters 10, 334 (1963).

R2 Roberts, R. W., Vanderslice, T. A., Ultrahigh Vacuum and its Applications (Prentice-Hall, New Jersey, 1963), pp. 85-86.

R3 Rowell, J. M., Kopf, L., Phys. Rev. 137, A907 (1965).

S1 Schrieffer, J. R., Scalapino, D. C., Wilkins, J. W., Phys. Rev. Letters 10, 336 (1963).

T1 Tinkham, M., Low Temperature Physics (Gordon and Breach, New York, 1961), p. 177.

T2 Townsend, P., Sutton, J., Phys. Rev. Letters 11, 154 (1963).